ABSTRACT

VASUDEVAN, BHARADWAJ. Assessment of Protection Schemes on a PV Dominated Distribution Feeder using HIL Testbed. (Under the direction of Dr. Mesut. E. Baran).

In this thesis, a Hardware-in-the-Loop (HIL) test bed has been developed to study the impact of Photovoltaics (PVs) on the protection system of a distribution feeder. The feeder under study has a large number of PVs and is called the Green Energy Hub (GEH). The HIL system uses a Real Time Digital Simulator (RTDS) to simulate the GEH. It also provides an interface to connect two protection relays. The relays provide overcurrent protection (51/51N) to the system. A series of tests have been conducted on this system to analyze and validate the findings reported in an earlier study which used PSCAD based simulation. Also the study has been extended to identify the problems faced in a fuse operated protection system in the presence of PVs. The study shows the difference between simulations based test studies and HIL test beds.

Assessment of Protection Schemes on a PV Dominated Distribution Feeder using HIL Testbed

by
Bharadwaj Vasudevan

A thesis submitted to the Graduate Faculty of
North Carolina State University
in partial fulfillment of the
requirements for the degree of
Master of Science

Electrical Engineering

Raleigh, North Carolina

2013

APPROVED BY:

_____	_____
Dr. Mesut. E. Baran Committee Co-Chair	Dr. Alex. Q. Huang Committee Co-Chair
_____	_____
Dr. David Lubkeman	

DEDICATION

To my parents, sister and her family.

To all those people who made a difference in my life.

BIOGRAPHY

Bharadwaj Vasudevan hails from a metropolitan city in India. He received a Bachelor's degree in Electrical and Electronics Engineering from the College of Engineering, Guindy, India in 2009. He was a Lead Electrical Engineer at Areva T&D designing electrical switchyards for transmission grids for 2 years before joining NC State University in 2011 for his Master of Science degree in Electrical Engineering. His research interests include Real Time Power System Simulation, Power System Protection and Automation, Computer networking, Mobile Computing and Radio electronics.

ACKNOWLEDGMENTS

Thanks to Mr. Jose Ruiz of ABB for helping with the setup of ABB Relion Relays.

Thanks to Dr. Juergen Holbach of Quanta Technology for providing the Omicron Amplifiers.

Thanks to Dr. Mesut E. Baran, my advisor, for his utmost guidance.

Thanks to Dr. Alex Huang for giving me the much needed opportunity.

Thanks to all my friends from 2352 for their moral strength.

Thanks to my parents for their patience and belief in me.

Thanks to Jason and Jon for the crucial final proof reading.

TABLE OF CONTENTS

LIST OF TABLES

LIST OF FIGURES

Chapter 1: INTRODUCTION

Centralized power generation has traditionally been the common model for electric power systems. With the advancements made in power electronic technology and increase in public awareness on the benefits of renewable energy, there has been an increase in the penetration of distributed energy resources (DERS) into the distribution feeder network. The inclusion of these devices, has subjected the conventionally radial system to have bi-directional power flow. The addition of DERs in the distribution feeders thus poses new design challenges. In addition to varying the power flow in the system, DERs also contribute during a fault. By doing so, they affect the operation of protective devices already present in the system. Hence modifications to the existing protection philosophies are needed to accommodate these discrepancies introduced by DERs in a distribution feeder.

1.1 Literature Survey

There has been a large amount of works published on the impact of Distributed Generators (DGs) on the protection of a distribution feeder. Listed below are issues highlighted in a few of these papers:

- **Under-reach at the feeder relay**- Addition of DGs on the feeder reduces the current sensed at the feeder relay location, reducing the distance covered by the protective device.[7][5][3]
- **Fuse coordination**- For a downstream fault, with the extra infeed from the DGs, fuses might blow before the recloser operates (failure of fuse-saving practice). Fuses might blow for an upstream fault for which they are not required to operate. Hence the coordination interval between the fuse and recloser might become smaller [3][5][8].
- **Sympathetic tripping** - Sympathetic tripping occurs when a protective device operates unnecessarily for faults in other protection zones. Such a tripping could be caused by the additional fault currents contributed from the DGs that were not

included in the original feeder protection design calculations for typical radial distribution systems. [3][5]

- **Feeding fault after utility protection opens**- The problems with unintentional islanding where DGs may inhibit arc extinction (if DG is not removed from the system within the first open interval of the recloser) and might make a temporary fault become a permanent fault. This could damage the devices in the system and introduce the problem of feeding to a fault even after the utility protection has cleared the fault. [6][5]
- **Impact on interrupting ratings of devices**- DRs can increase the amount of fault current flowing through the utility breaker, recloser and fuse, especially when synchronous generators are in close proximity.[3][8]
- **Ground source impact**-DGs should not source any ground current, as the ground fault relays on the utility side are very sensitive and may cause unnecessary tripping.[3]

Some of the papers proposed a few techniques to suppress these issues. They are listed below:

- Employing a modified Direct Transfer Tripping based Protection scheme between relays in the distribution feeders[5]
- Implementing an adaptive over current protection for feeders [7].
- Adjusting the relay protection parameter settings to accommodate the reduction in reach caused by PVs.[1]
- In a special condition where SSTs are available in the system, the use of communication techniques in SSTs, the fault current contributed by DERs is calculated and fed into the relay.[1]

Though various mitigation techniques have already been proposed in [1], they were all tested on a fully simulated environment using software like PSCAD. Such an approach has its own

limitations. As with PSCAD, it is primarily a tool for analyzing transient responses of electric power systems. It does not have the flexibility of incorporating real equipment (Intelligent Electronic Devices - IEDs) in testing, thus eliminating the possibility of evaluating the electrical system and protection equipment simultaneously. We seek to overcome this limitation by using hardware in the loop (HIL) system in which protection devices have been connected to the simulator to form a closed-loop to interact with the simulated power circuit. We intend to analyze and confirm the findings reported in [1] in this test bed developed. Dr. Hossein had also proposed in [1], a procedure to implement his mitigation technique. We have verified this procedure by conducting it in our test bed. We have also incorporated fuse models in RSCAD platform and performed an impact study to identify all the worst case scenarios. The need for HIL systems to conduct these studies has been justified in the end.

Chapter 2: A Hardware-in-loop test bed for assessment of Distributed Feeder Protection

This chapter provides details about the HIL system used in our study. The main components of the HIL are shown below Figure 1.

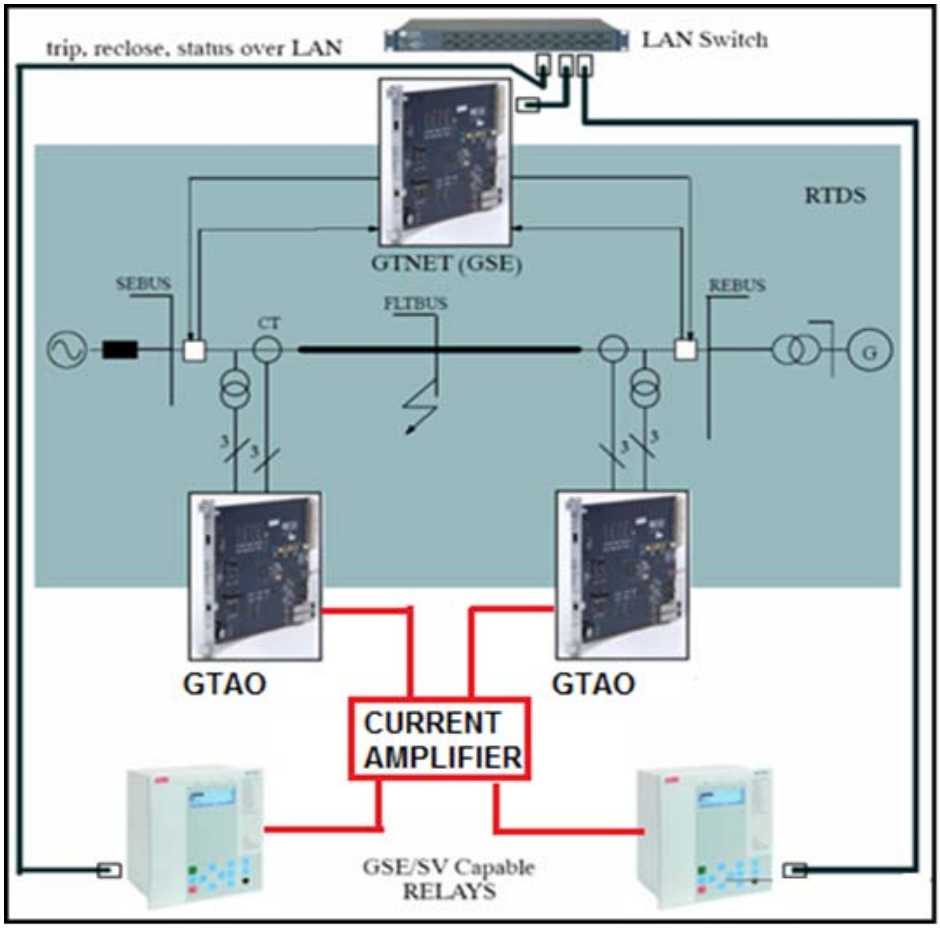

Figure 1 RTDS Hardware in the loop test bed

As shown in Figure 1, the main components of a HIL system include:

1. Real Time Digital Simulator(RTDS)
2. Analog Interfaces
3. Current Amplifier
4. Relays.
5. Communication interfaces

Each of these components is explained below.

2.1 Hardware in the Loop Components

2.1.1 Distribution System Simulation in RTDS

Figure 2 shows the single line diagram of the notional feeder circuit used as a prototype test feeder in [1]. This circuit has two feeders supplied from the substation transformer. The two feeders belong to the 15 kV class and operate at a nominal voltage of 12.47 kV. Lumped loads have been connected to the feeder at various nodes after the substation transformer. Explicit load data and ratings of the connected devices are provided in appendix 1.

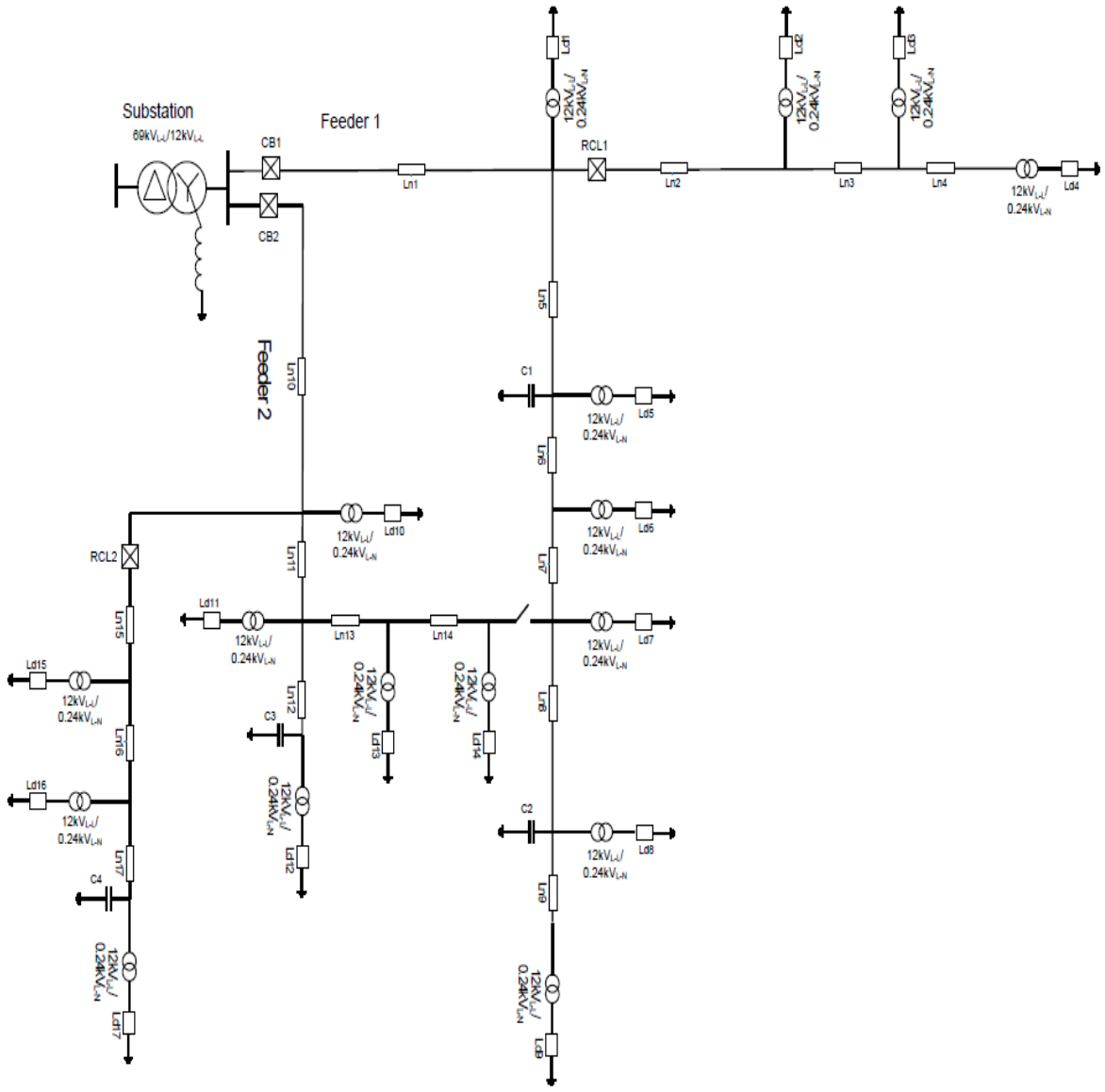

Figure 2 PSCAD version of the actual distribution feeder

With the advancements made in PV technology, there has been a continuous increase in the penetration of PV panels in the average household. Therefore an appropriate representation

of feeders in the near future would include PVs attached with load units at their nodes. The circuit in Figure 2 has been thus converted into a PV based residential Green Energy Hub (GEH) feeder system, in which a Distributed Energy Resource (DER) is attached to each of the load nodes as shown in Figure 3. The DERs' capacity is matched to the maximum load available at the respective nodes.

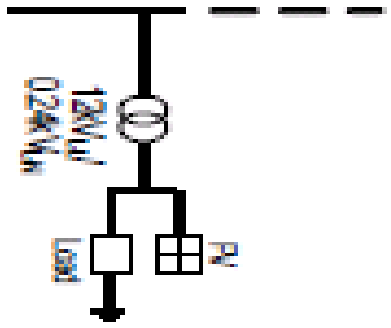

Figure 3 A node of Green Energy Hub

Further, in Chapter 3 of [1], it was shown that the presence of DERs upstream to a protection device does not hinder the operation of the protective devices. All these considerations were taken into account for modeling the new system in RSCAD. Therefore, the second feeder coming out of the substation was removed. The final circuit included one main outgoing feeder from the substation and one lateral upstream to the recloser. At each load node we have introduced PVs as depicted in Figure 3. The modified circuit is shown below in Figure 4. In this system the line sections are all nominal pi models. It is worth noting that the

transformer model available in RSCAD does not make allowances for no load losses. Since the impact of no load losses in our fault study is negligible, this is not expected to affect the results of the simulation significantly. The same shall be verified in the later sections. CT models have been used to provide secondary currents to the GTAO cards of RTDS for interfacing with the external relays.

2.1.2 Grid Connected PV System in RTDS:

Figure 5 shows all the main components of the PV model used in PSCAD. In this model each of the components shown has been explicitly modeled, thus making them computationally complex. The modeling details are available in [1].

A simplified model was developed for RSCAD to accommodate for the space constraints in RTDS. One of the primary modeling requirements in RTDS was computational simplicity to simulate large systems within a given hardware. RTDS technologies recommend that for a system to replicate a real time scenario, it has to be run at a time step close to 50µs. Thus the model adopted for RTDS simulations was computationally less intense and allowed us run the system at 70 µs time step. The components of the RSCAD PV system are shown in Figure 6.

In this system, the model for PV was developed by Mr. Nicholas Brooks Parks in "Black Start Control of a Solid State Transformer for Emergency Distribution Power Restoration" [15]. From [15], base equations for calculating the current reference output of a PV as a function of solar insolation have been adopted into the RSCAD model.

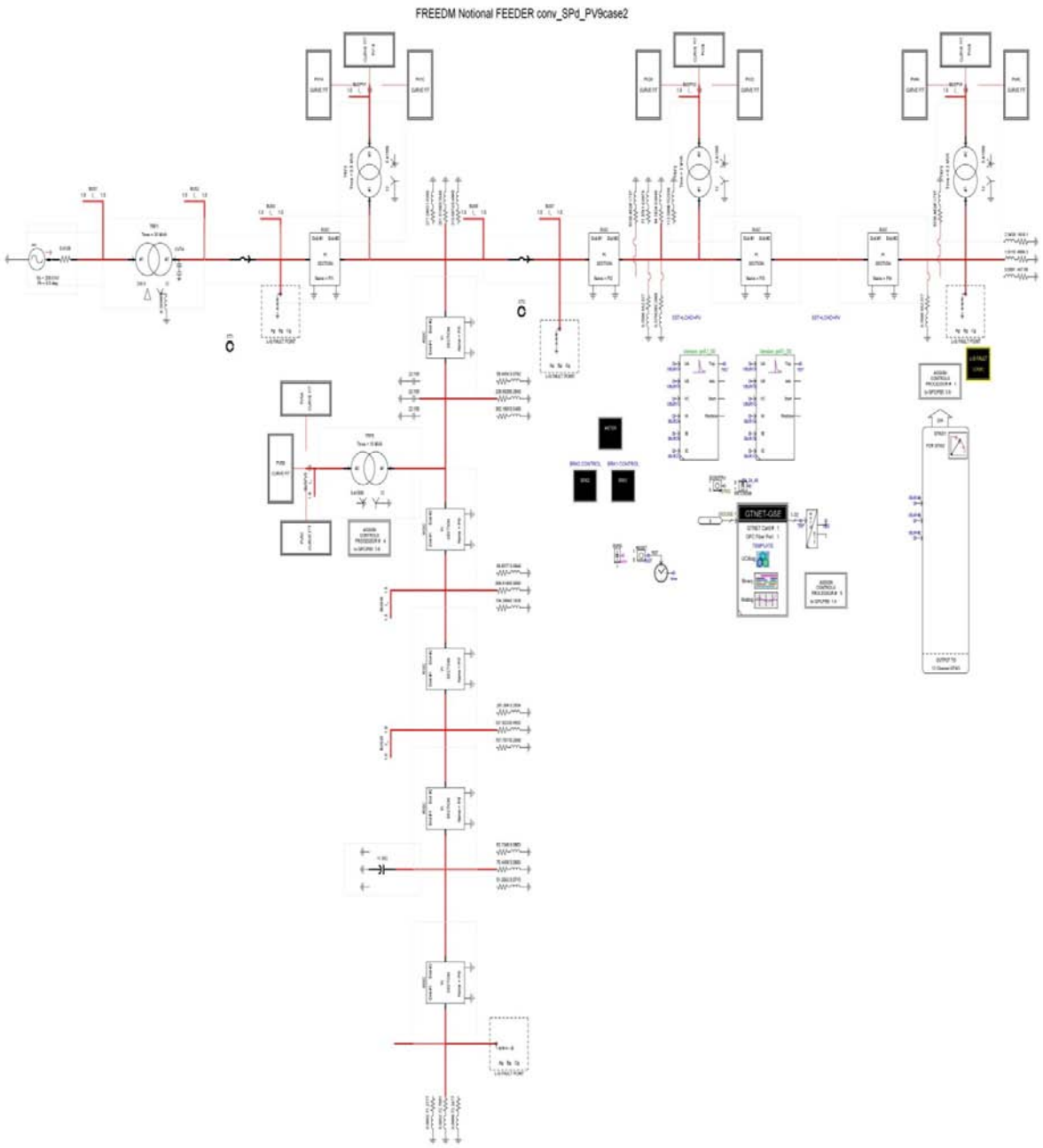

Figure 4 RSCAD model of the Green Energy Hub circuit

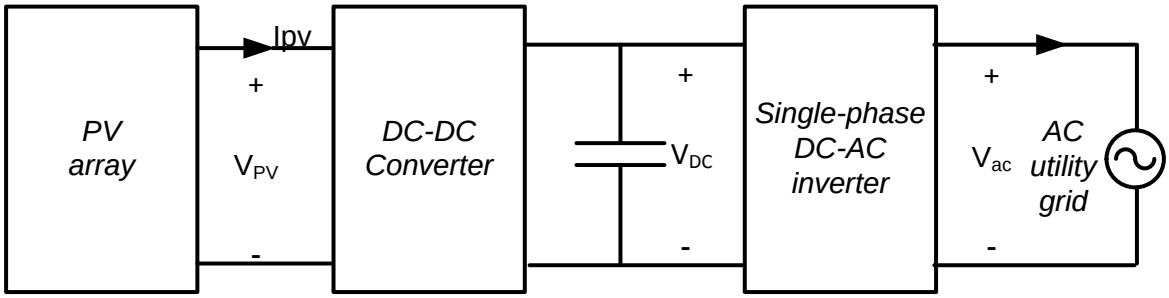

Figure 5 Main components grid connected PV system in PSCAD

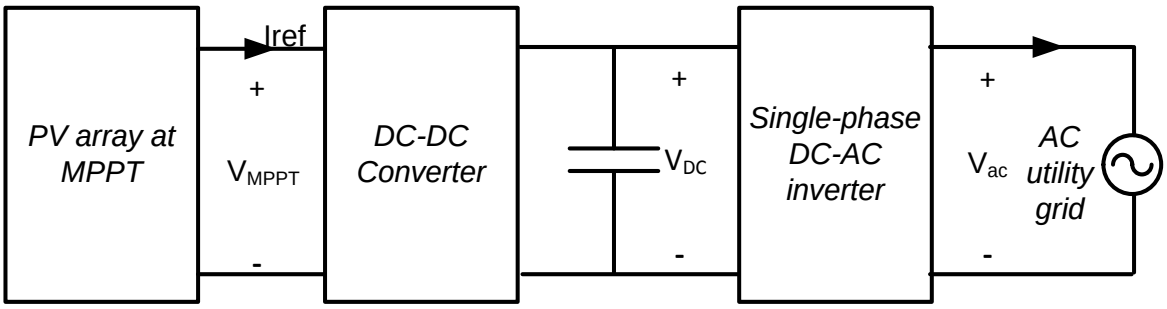

Figure 6 Hybrid PV Model in RSCAD

It can be seen that the major difference between the PSCAD model and the RSCAD model is that the PV system in RSCAD comprises a PV panel always operated at Maximum Power Point (MPP). This reduces the computations required in HIL simulations. The design procedure to calculate the operating point is available in appendix 2.

Based on the parameters for the PV, the MPPT voltage is approximated as a function of solar irradiation using the following formula:

$$V_{MPPT} = \frac{W(ae) - 1}{b}$$

Where $a = [I_{scr} + K_\theta(T - T_r)]\frac{S}{100I_{rs}} + 1$, $b = \frac{qv_{dc}}{kTAn_s}$ and W is the Lambert function.

In this equation the solar insolation S is the independent quantity. The rest of the terms in a, Iscr (Short circuit current) K_θ(Temperature Coefficient) Irs (Reverse Saturation Current) are all constant parameters specific to a PV panel. The term b includes the diode constant and v_{dc}. In our case we have assumed v_{dc} to be 1V. Detailed information about these parameters is available in appendix 2. For the PV system used in RSCAD, the calculated values for V_{MPPT} has been plotted against the solar insolation (S) in Figure 7.

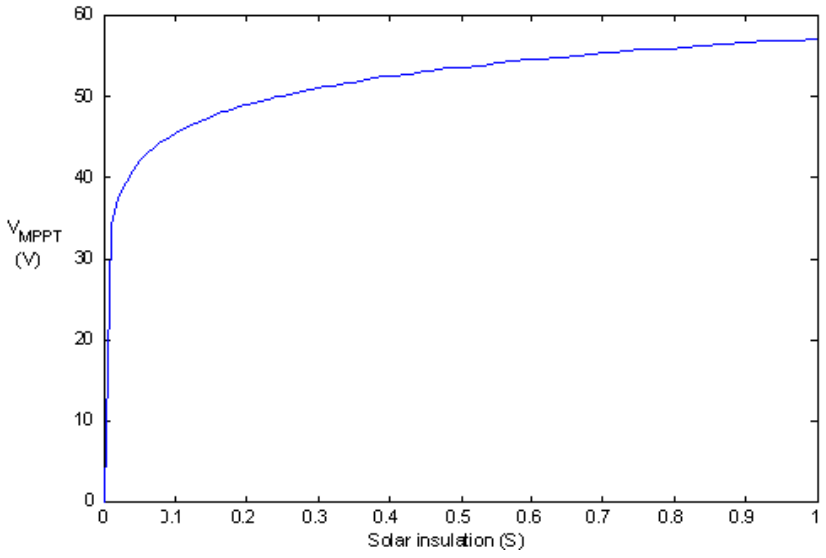

Figure 7 PV module Characteristics

This curve was represented as a seventh order polynomial equation in RSCAD as shown below.

$$y = p(0) * x^7 + p(1) * x^6 + p(2) * x^5 + p(3) * x^4 + p(4) * x^3 + p(5) * x^2 + p(6) * x + p(7)$$

The coefficients $p(0) \ldots . p(7)$ are collected from the polynomial curve fitting algorithm (refer Fig 11). This equation is implemented as a C script in RSCAD. The script file is available in appendix 2. The values of $p(0) \ldots . p(7)$ are given in Figure 8.

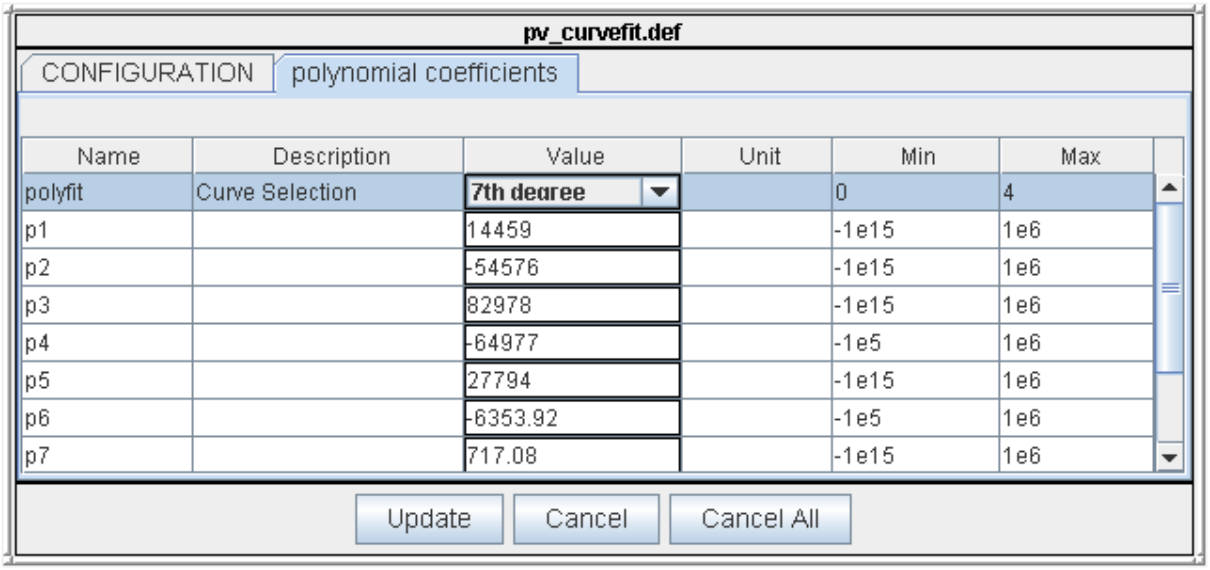

Figure 8 Parameter settings for PV component in RSCAD

The curve fitted PV characteristics is shown in Figure 9.

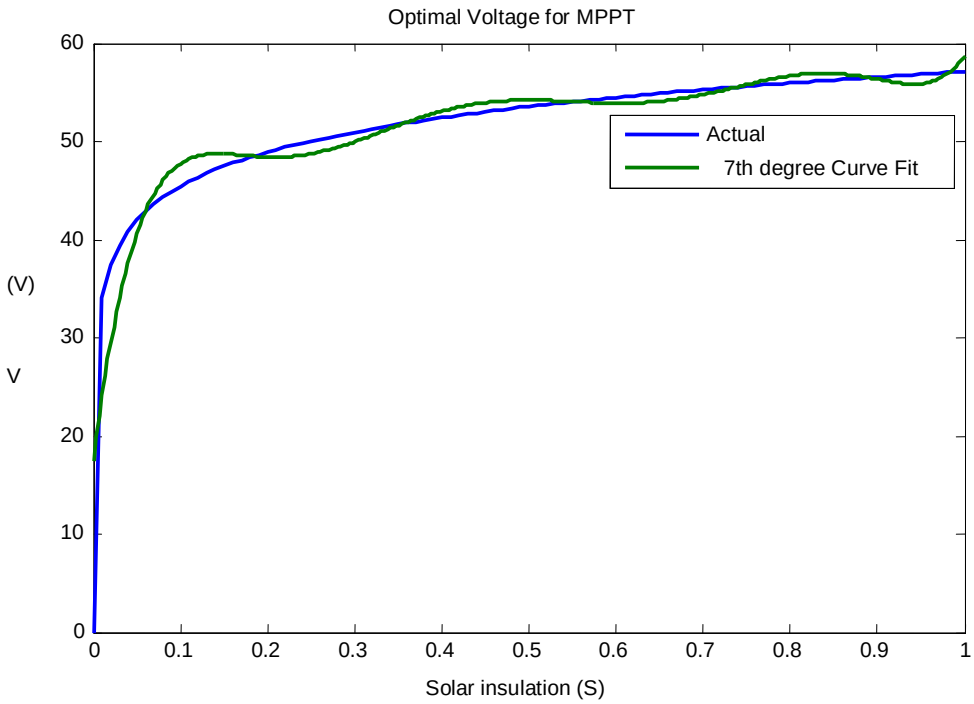

Figure 9 Curve fit for the optimal voltage reference curve

2.1.3 RTDS Interfaces

The RTDS hardware has various interfaces to connect to the external devices. These interfaces are in the form of cards namely, GTAI/GTAO (for Analog I/O), GTDI/GTDO (for Digital I/O) and GTNET (for IEC 61850 communications). In our HIL system we have specifically used the GTAO and GTNET cards for the data transfer. The feeder circuit model

simulated in RSCAD provides the necessary signals that are to be transferred via the HIL loop as shown in Figure 1. Similarly the RSCAD simulation also contains inputs which collect data from the external world. These interface connections are explained in detail below:

- **Analog Outputs**: The CT outputs (X1) from RSCAD simulations are collected from the RTDS via the GTAO cards (X2), as shown in Figure 10. These outputs are low voltage signals from RTDS with a peak value set at 10V. These raw signals need to be scaled in order to be interfaced with an amplifier, since the amplifier itself has its own gain.

Figure 10 RTDS analog output setup from GTAO card

As per RTDS guidelines the GTAO output should not exceed 5V. This is achieved by controlling the scaling factor (SCL) in GTAO cards. The SCL is thus calculated using the formulae shown below.

$$X_1 \times \frac{5}{SCL\_I} = X_2 \quad (1)$$

$$X_2 \times K_1 = X_3 \quad (2)$$

The output of the amplifier should match the CT secondary inside RTDS. Hence

$X_1=X_3$, Therefore **$SCL_{-1}=5\times K1$**

- **Network Communication Interface:** The GTNET card (Figure 11) in RTDS provides the network interface between the relay and the simulation system in RTDS. The binary input points from the GTNET card (TRP) as shown in Figure 11 serves as an input to the breaker tripping logic. As in a typical real world scenario, a control unit has been simulated in RSCAD for interfacing the trip signal to the breaker. This unit also communicates back via (GOOSE1) in Figure 11, the status of the breaker to the relay for safe operation of the relay.

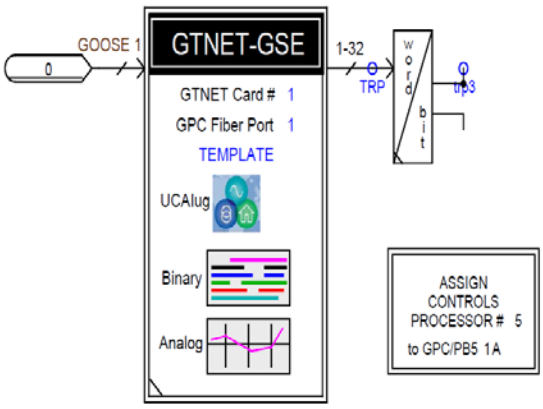

Figure 11 GTNET card in RSCAD

2.1.4 Protection Relays

The amplifier output (X3) shown in Figure 10, provides the secondary current injection for the relay. Based on the scaled output from the GTAO card of the RTDS, the amplifier

provides current into the analog input of the relay. The overcurrent protection inside the relay makes its decision and when required sends a trip signal as an IEC61850 based Generic Object Oriented Substation Event (GOOSE) message via the front ethernet port. GOOSE is a peer-peer messaging technology typically used in a substation environment for exchanging event triggered decisions between two relays. In this study we have used two ABB Relion relays to implement the protection functions. The following system engineering tools from ABB were used to configure the relay settings for our HIL system:

- **PCM 600**[1] **-** The application configuration and protection parameter settings for the numerical relays are created using this software. For our system the time delayed over current protection for both phase and ground faults have been used in the relay. The application configured is shown below in Figure 12. It can be seen that each of the protection function is modeled as functional block in PCM600. The parameter settings associated with these blocks are attached in appendix 3.

[1] Product of ABB Inc.

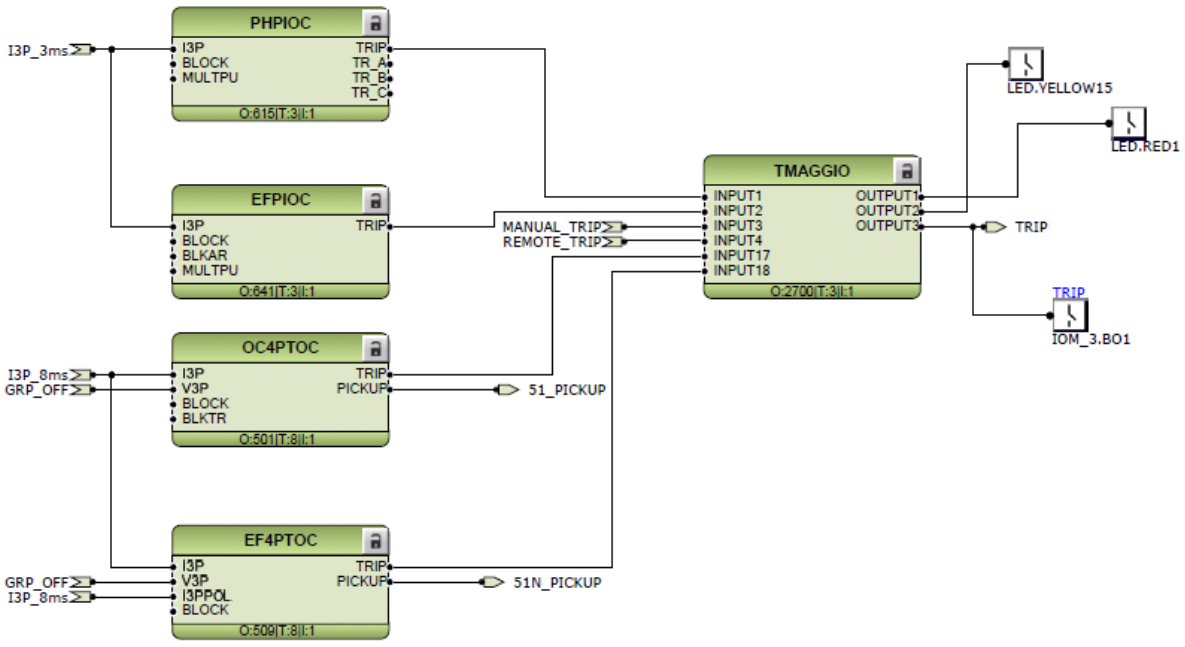

Figure 12 Functional block configuration for 51/51N protection[1]

- **IET 600[1]** - The IEC61850 communication settings for GOOSE message broadcast is setup using this software. The output signals available from the protection functional blocks modeled in PCM600 are used in this software to create goose datasets. They are then embedded into a GOOSE control Block (GCB). As per the IEC61850 standard every GCB is encapsulated into the GOOSE packets. These GCBs are used by other peers (in our case, the RTDS GTNET card) to subscribe to the publishing relay to receive these GOOSE packets. The complete information about the GOOSE subscription and also the protection settings are available as .SCD file that can be exported from this software [14].

- **SCD Editor in RSCAD[2] -** The Substation Configuration Description (SCD) file from the relay is of XML format and includes all the information regarding the application modeled in the relay. This file is imported into the SCD editor of RTDS. The process objects corresponding to the trip signal from the relay which is available inside the published GCB (visible in the .SCD file) is mapped to the one of the 32 binary inputs (TRP in Figure 11) of the RTDSs' GTNET card. This binary input is then used to trip the breaker.

2.1.5 Relay Settings in RSCAD

In our HIL system ABB Relion REC670 relays interact with the system in the RTDS to provide overcurrent (51/51N) protection. The settings for these relays were obtained from the PSCAD equivalents in [1]. The relay model used in PSCAD had two stages of over current protection for both phase and ground relays. The following were its settings:

BRK1 Settings:

1. Phase relaying, first operation: pickup = 1440 amps, Schweitzer "U5" curve, time dial 1.1

2. Phase relaying, second operation:pickup = 1440 amps, Schweitzer "U5" curve, time dial 1.1
3. Ground relaying, first operation: pickup = 480 amps, Schweitzer "U5" curve, time dial 1.8
4. Ground relaying, second operation:pickup = 360 amps, Schweitzer "U3" curve, time dial 4

[2] Product of RTDS Technologies.

RCL1 settings:

1. Phase relaying, first operation: pickup = 1200 amps, ABB PCD 2000 Short Time inverse curve, time dial 0.844
2. Phase relaying, second operation: pickup = 600 amps, ABB PCD 2000 Extremely inverse curve, time dial 1
3. Ground relaying, first operation: pickup = 480 amps, ABB PCD 2000 Short Time inverse curve, time dial 1.467
4. Ground relaying, second operation: pickup = 240 amps, ABB PCD 2000 Extremely inverse curve, time dial 4.11

Since the curves used in the PSCAD version were not compatible with the ABB relays, a curve fitting was done to define a setting closely in match with the actual settings in PSCAD. Based on that the relay settings on the ABB relays were chosen as follows:

BRK1 Modified Settings:

1. Phase relaying, first operation: pickup = 1460 amps, ANSI Normal Inverse curve, time dial 0.36
2. Ground relaying, first operation: pickup = 480 amps, ANSI Normal Inverse curve, time dial 0.822

RCL1 Modified Settings:

1. Phase relaying, first operation: pickup = 1245 amps, ANSI Normal Inverse curve, time dial 0.12
2. Ground relaying, first operation: pickup = 480 amps, ANSI Normal Inverse curve, time dial 0.295

The second shot for the relay was not implemented in the HIL system since the PV's impact for a fault would be present only up to the first shot of the relay. Since the second shot is a slow curve, the relay will operate only after all the PVs have shut down.

Figure 13 and

Figure 14 compare the inverse time characteristics of the ABB relay and the PSCAD relay models. Additionally the relays were also modeled within the RSCAD and the same PSCAD settings were implemented in the relay models.

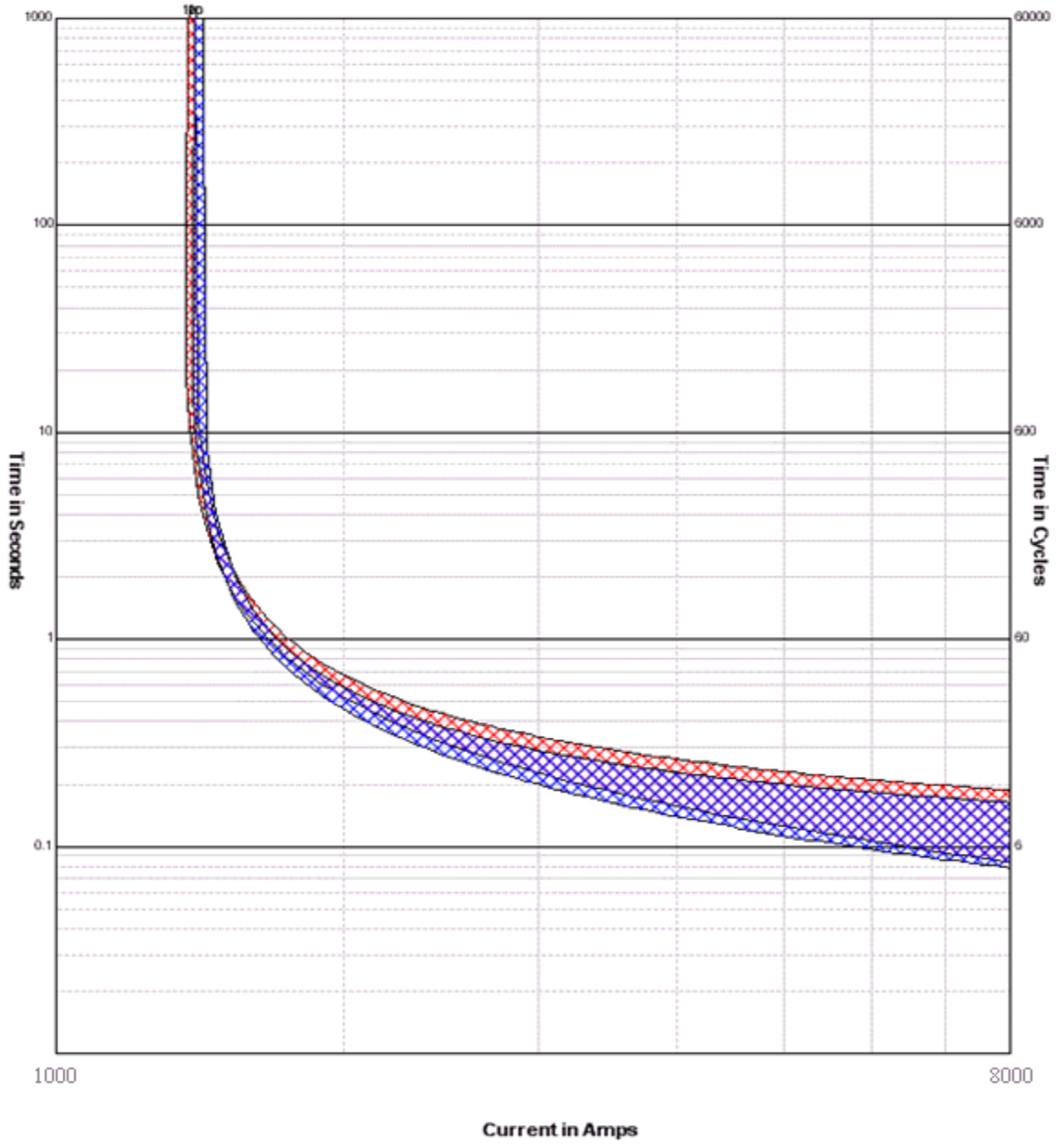

Figure 13 Inverse Time Characteristics of BRK curves from PSCAD Relay model (RED) and ABB Relay (BLUE)

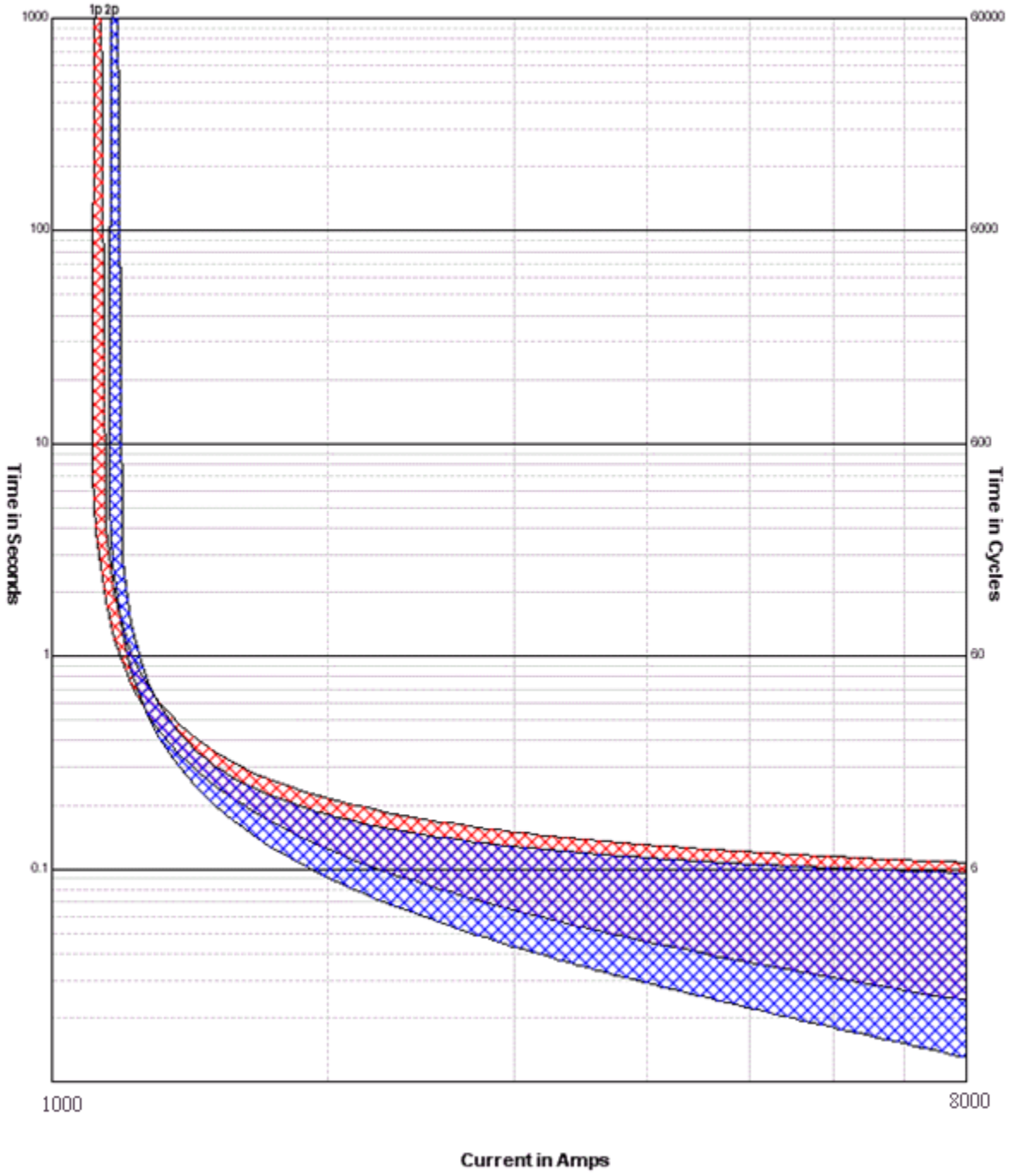

Figure 14 Inverse Time Characteristics of RCL curves from PSCAD Relay model (RED) and ABB Relay (BLUE)

Shown below in Table 2.1-a & b is a comparison chart of the fault current and corresponding relay operating time, for actual ABB relays, RSCAD and PSCAD models. The bolted fault case has been considered in two scenarios - with and without PVs and the settings was checked for the fault clearing time (FCT).

Table 2.1-a Fault Clearing Time (FCT) of BRK & RCL in PSCAD, RSCAD & ABB Relay for 3ph Fault w/o PV

No PV

	FCT(s)					
	3ph Fault(kA)	RTDS	3ph Fault(kA)	ABB	3ph Fault(kA)	PSCAD
RCL	3.3	0.0927	3.047	0.092	3.195	0.234
BRK	2.322	0.379	2.252	0.399	2.299	0.404

No PV

	FCT(s)					
	1ph Fault(kA)	RTDS	1ph Fault(kA)	ABB	1ph Fault(kA)	PSCAD
RCL	1.904	0.1937	1.735	0.128	1.958	0.25
BRK	1.173	0.435	1.153	0.451	1.169	0.367

Table 2.1-b Fault Clearing Time (FCT) of BRK & RCL in PSCAD, RSCAD & ABB Relay for 1ph Fault with PV

With PV

	FCT(s)					
	3ph Fault(kA)	RTDS	3ph Fault(kA)	ABB	3ph Fault(kA)	PSCAD
RCL	3.169	0.0908	3.185	0.0841	3.394	0.0803
BRK	2.302	0.3992	2.296	0.406	2.3	0.4109

With PV

	FCT(s)					
	1ph Fault(kA)	RTDS	1ph Fault(kA)	ABB	1ph Fault(kA)	PSCAD
RCL	1.918	0.12045	1.878	0.125	1.968	0.12
BRK	1.214	0.406	1.178	0.441	1.223	0.35

It is evident from the results in Table 2.1-a and Table 2.1-b that the models are adequately accurate. For e.g., consider the 1ph fault with the PV scenario, the BRK relay model in RSCAD trips at 1.214 secs, while the ABB relay and PSCAD relay trips at 1.178 and 1.223 secs.

2.2 Verification of Test Feeder Simulation

In the previous section, the individual components of the green energy hub system modeled in RSCAD, have been discussed and verified against their PSCAD equivalents. In this process, we came across a number of approximations and modeling limitations for the different components. In order to validate the system modeled in RSCAD, we need to compare the performance of this system with that of the PSCAD system. This is achieved by matching the steady state and fault currents seen by the protective relays in both systems.

The waveforms captured by the relay for a three phase (3ph) and single phase (1ph) bolted fault at the end of the feeder is shown in Figure 15 & Figure 16. The PSCAD equivalents are attached below in Figure 17 & Figure 18.

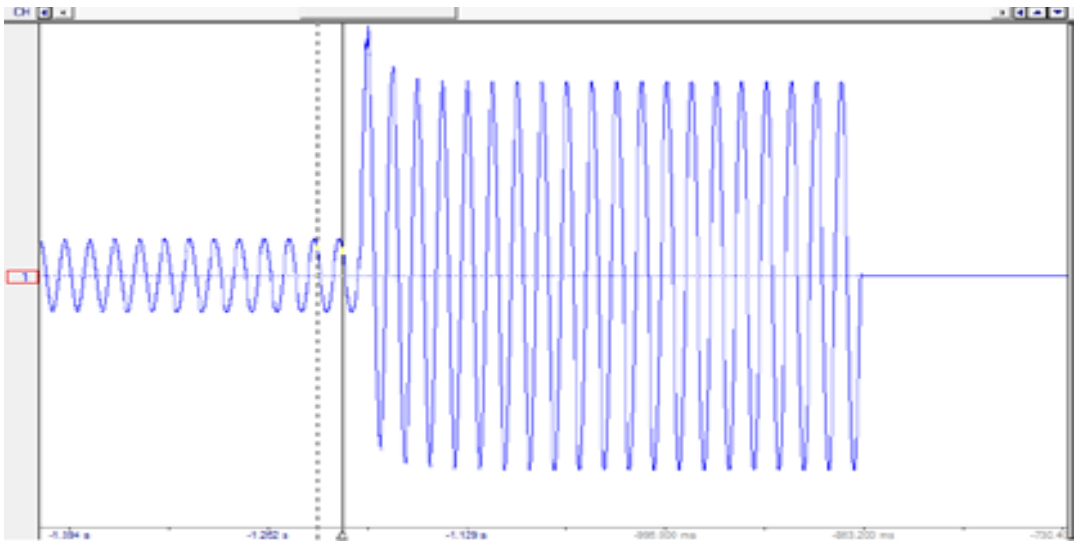

Figure 15 I ph A Fault Current 3ph bolted fault far from the Breaker without PV

The steady state current measured by BRK and RCL for phase A in the presence of PVs was 436A (rms) and 84A (rms) respectively in RSCAD. The same was measured in PSCAD as 432A (rms) and 83A (rms). For the case shown in Figure 15, PSCAD fault current measurement was BRK: 2.299kA (rms) as shown in Figure 17. In Figure 19 the same was measured as 2.18kA in RSCAD.

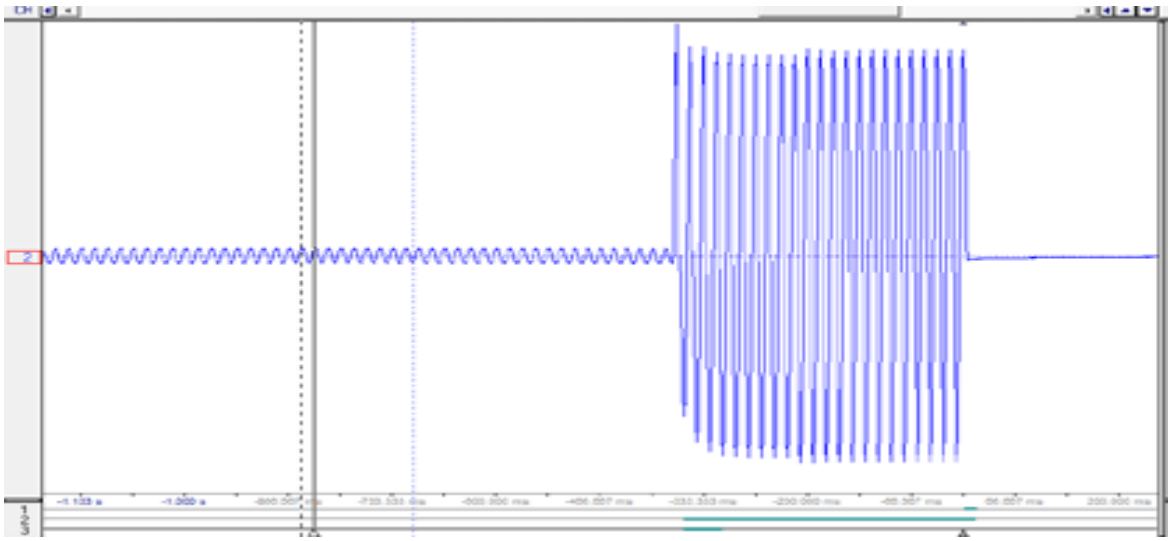

Figure 16 I ph A Fault Current 3ph bolted fault far from the Breaker with PV

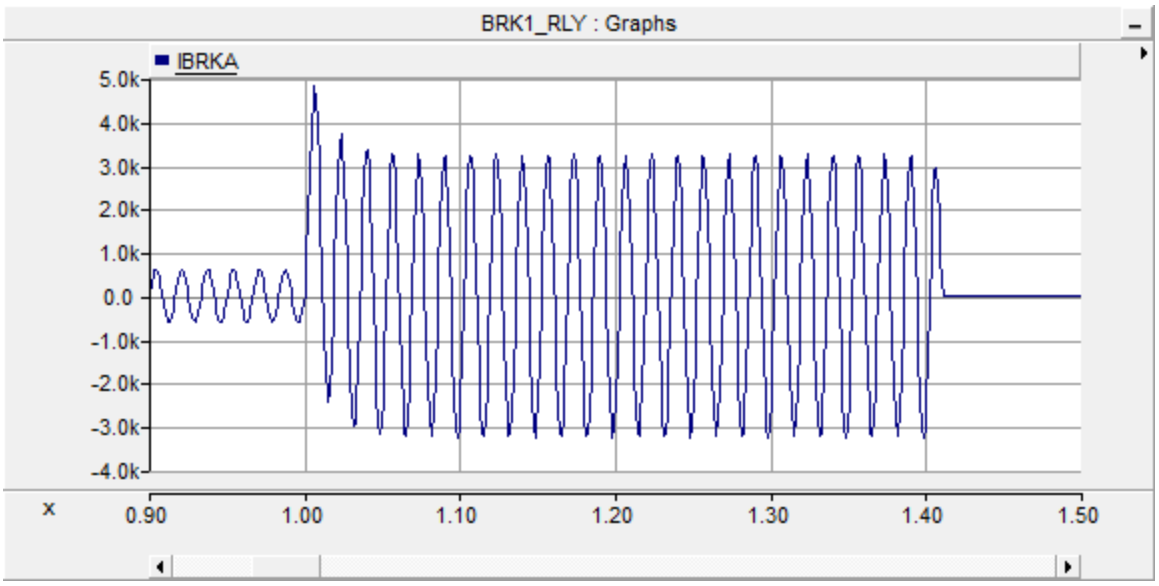

Figure 17 I ph A Fault Current 3ph bolted fault far from the Breaker without PV from PSCAD

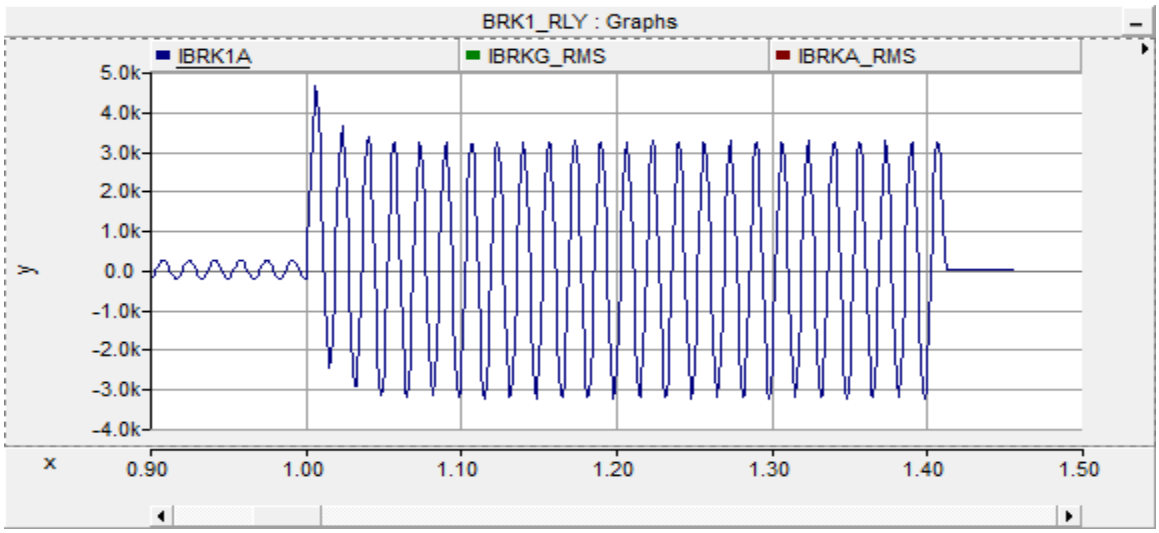

Figure 18 I ph A Fault Current 3ph bolted fault far from the Breaker with PV from PSCAD

Figure 19 and Figure 20 shows the fault currents seen by the relay models in RSCAD. For a 3ph bolted fault in the presence of PVs, it's seen that the RSCAD relays measured 2.2kA as shown in Figure 20.

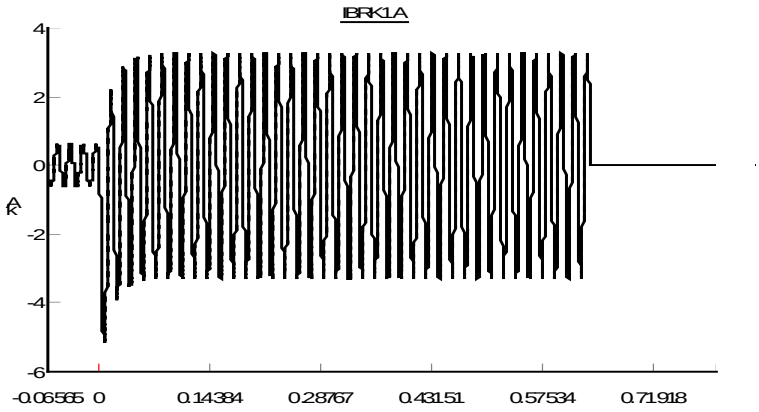

Figure 19 IphA Fault Current 3ph bolted fault far from the Breaker without PV in RSCAD

Figure 20 IphA Fault Current 3ph bolted fault far from the Breaker with PV in RSCAD

Figure 21 & Figure 22 shows the neutral current captured by the relay for a 1ph fault. The Analog outputs from the GTAO card of RTDS are scaled only to certain accuracy. Hence there comes a need to verify the curves seen by the relay to the ones generated by the RTDS. When compared with the RSCAD simulation results from Figure 23 & Figure 24, both of them measured a fault current of 1.98kA in the presence of PVs.

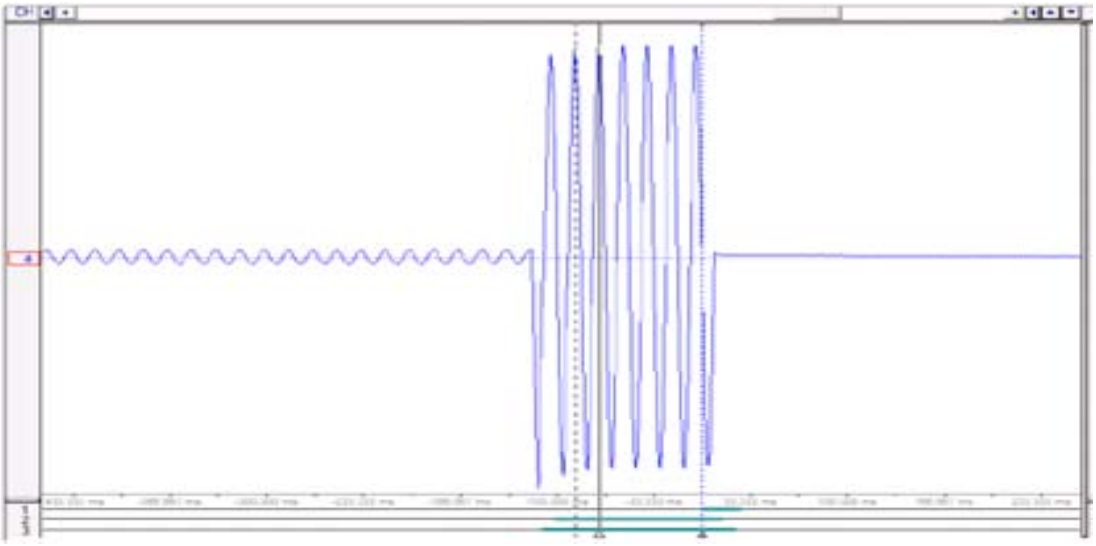

Figure 21 IN Fault Current 1ph bolted fault far from the Recloser without PV

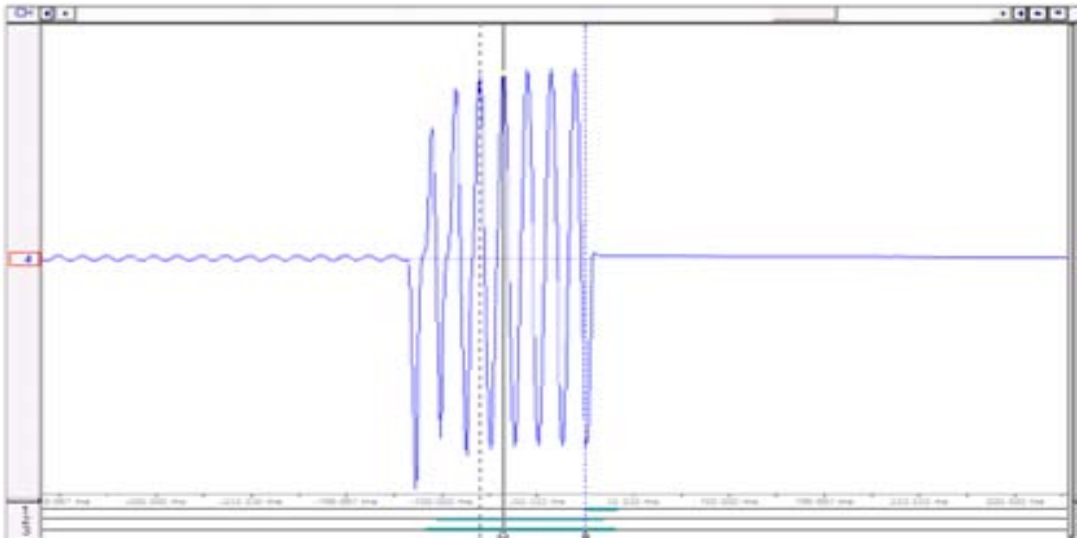

Figure 22 IN Fault Current 1ph bolted fault far from the Recloser with PV

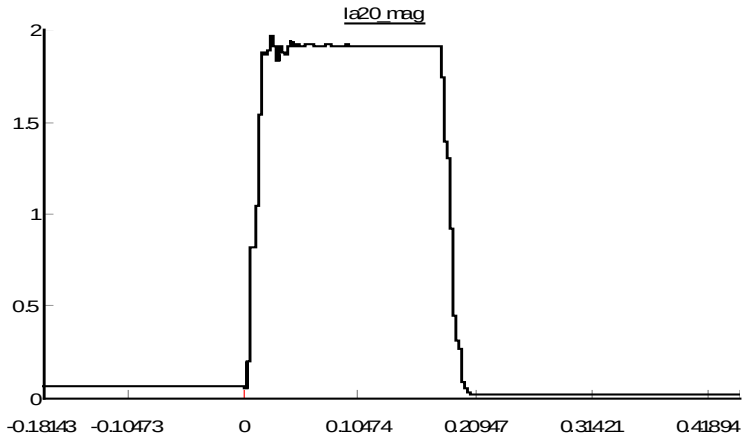

Figure 23 IN RMS Fault Current 1ph bolted fault far from the Recloser without PV in RSCAD

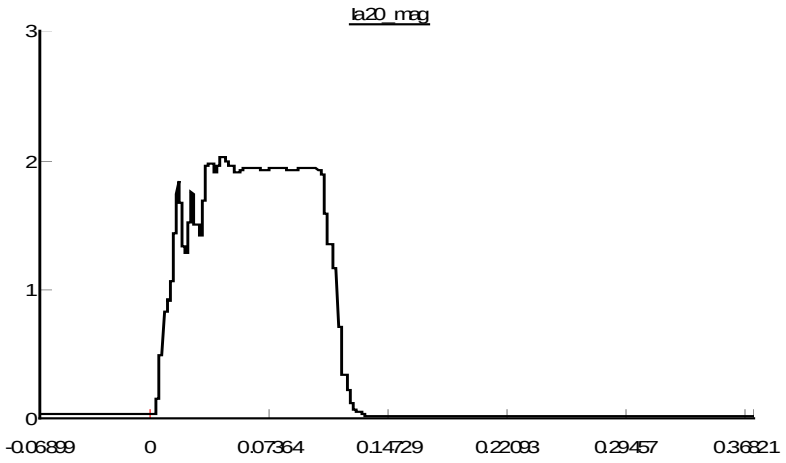

Figure 24 IN RMS Fault Current 1ph bolted fault far from the Recloser with PV in RSCAD

The comparison of the steady state and fault simulation results from PSCAD and RTDS verifies that the system model implemented in the RTDS has an error limit of 5% approximate for fault currents and a 2% error limit for steady state currents. Even the relay operating times are within the 5% error limit when compared with the PSCAD relay models. These results indicate that the HIL performs satisfactorily and can be used to replicate the PSCAD simulation test cases.

Chapter 3: Impact of PVs on Distribution feeder protection

Dr. Hossien in [1] conducted a comprehensive study on the impact on the feeder protection in a PV dominated distribution feeder. He identified two main issues on the feeder protection as change in reach and operating time of the relays due to the presence of PVs in the system. Using the HIL test bed, we have repeated a few test cases from [1] to verify the identified issues.

3.1 Change in reach and operating time of the protective relays

In chapter 1, it was stated that Distributed Energy Resources (DERs) present downstream to the protective relays could potentially source enough fault current so that the protective relay would not see the fault. Therefore downstream PVs had a greater impact on the reach and operating time of the relays. A typical contingency that causes under reach in a PD due to the presence of DGs downstream of it is shown in Figure 25. The DG could possibly source enough fault current that the fault goes undetected by the PD.

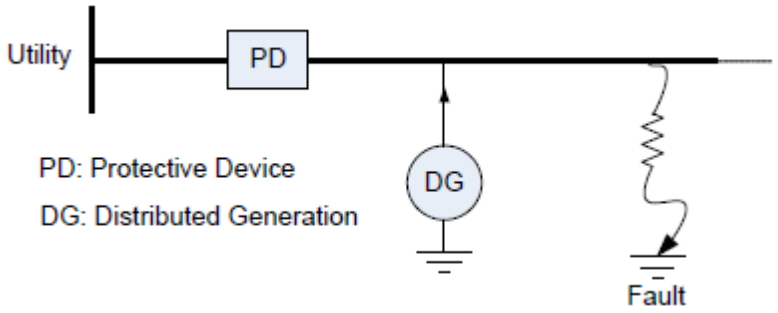

Figure 25 Change in PDs' current due to the presence of DER

It was identified in Dr. Hossein's thesis that the operating time of the protective relay is mainly affected by the following:

1. Amount of PV Generation
2. PVs' Location
3. Fault Resistance
4. Fault Location

To validate these problems, we replicated the test scenario detailed in [1]. A series of test cases were conducted in the HIL testbed by varying all the above mentioned parameters to get a complete assessment of the protection scheme in operation. For these tests, the amount of PV generation is expressed as a percentage of the system load. A 50% power output of the PV means the PVs contribute to 50% of the system load. All PVs were located downstream of the Protective Relay. For the fault resistance various values were considered to determine the worst case scenario.

Two types of faults viz., 1 phase (1ph) and 3 phase (3ph) faults were used to conduct this study. The four fault locations (F1, F2, F3, and F4) have been shown in the Figure 26, Single Line Diagram of the GEH in RSCAD.

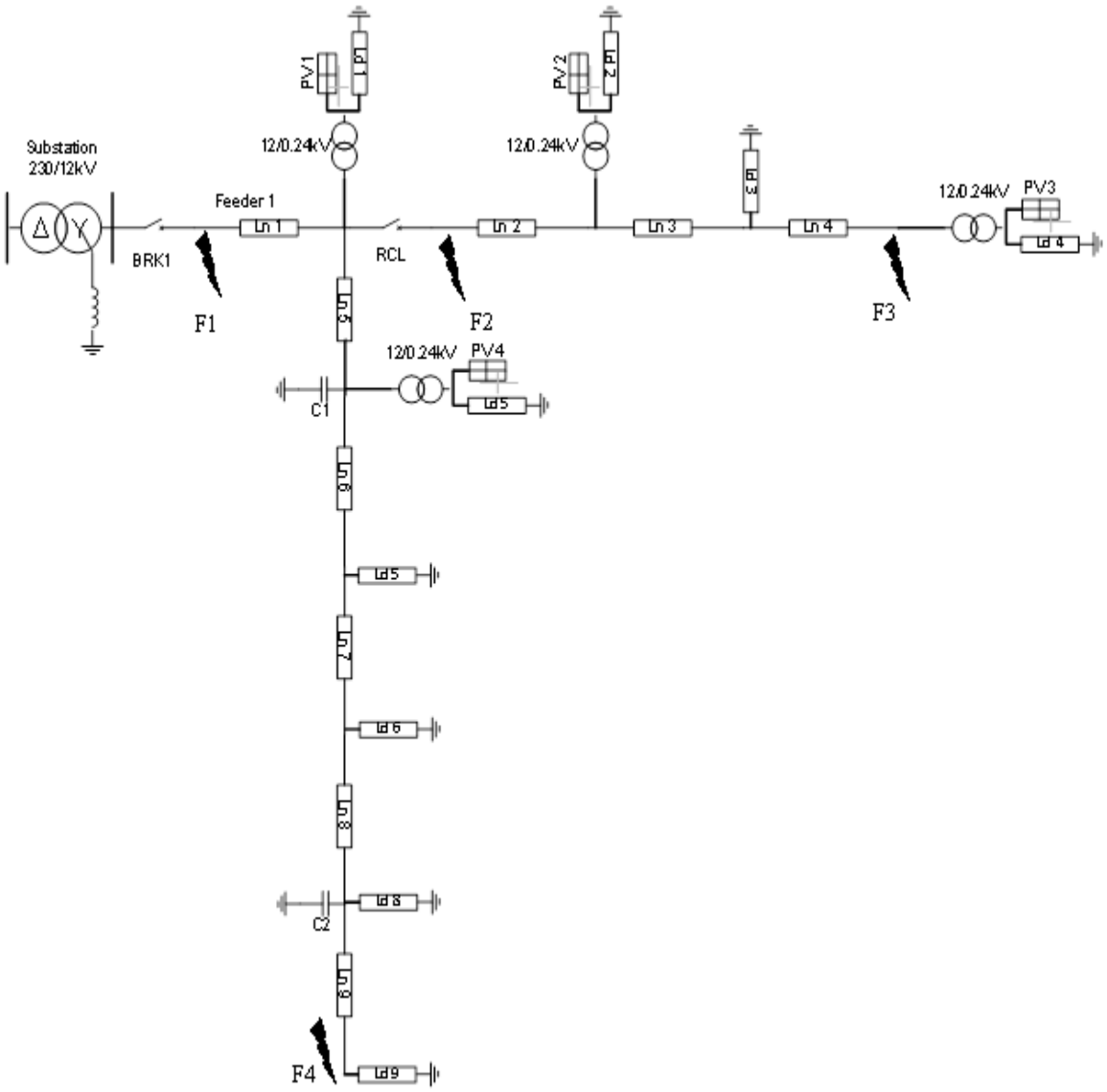

Figure 26 Single line diagram of the Green Energy Hub in RSCAD

3.1.1 Test Results

For this study, PVs have been aggregated in four locations at the line section after Ln 1, Ln 2, Ln 4 and Ln 6 as shown in Figure 26. By this arrangement we have all the PVs downstream to the breaker (BRK1). For the recloser (RCL) we have more PVs upstream of it than those downstream. Hence this system represents a case with DGs downstream of a PD which is also the worst case specified before in [1].

For each test case fault was placed on the aforesaid points and the time of operation of the relay was measured from the COMTRADE file obtained from the relay. This file contains the complete information of the fault current waveform. All these files are available at [12]. The collected data is summarized in the form of plots shown below.

1. ***Breaker Distant faults***

Fig 27 and 28 summarizes the effect of PVs on the operating of the breaker on the main feeder.

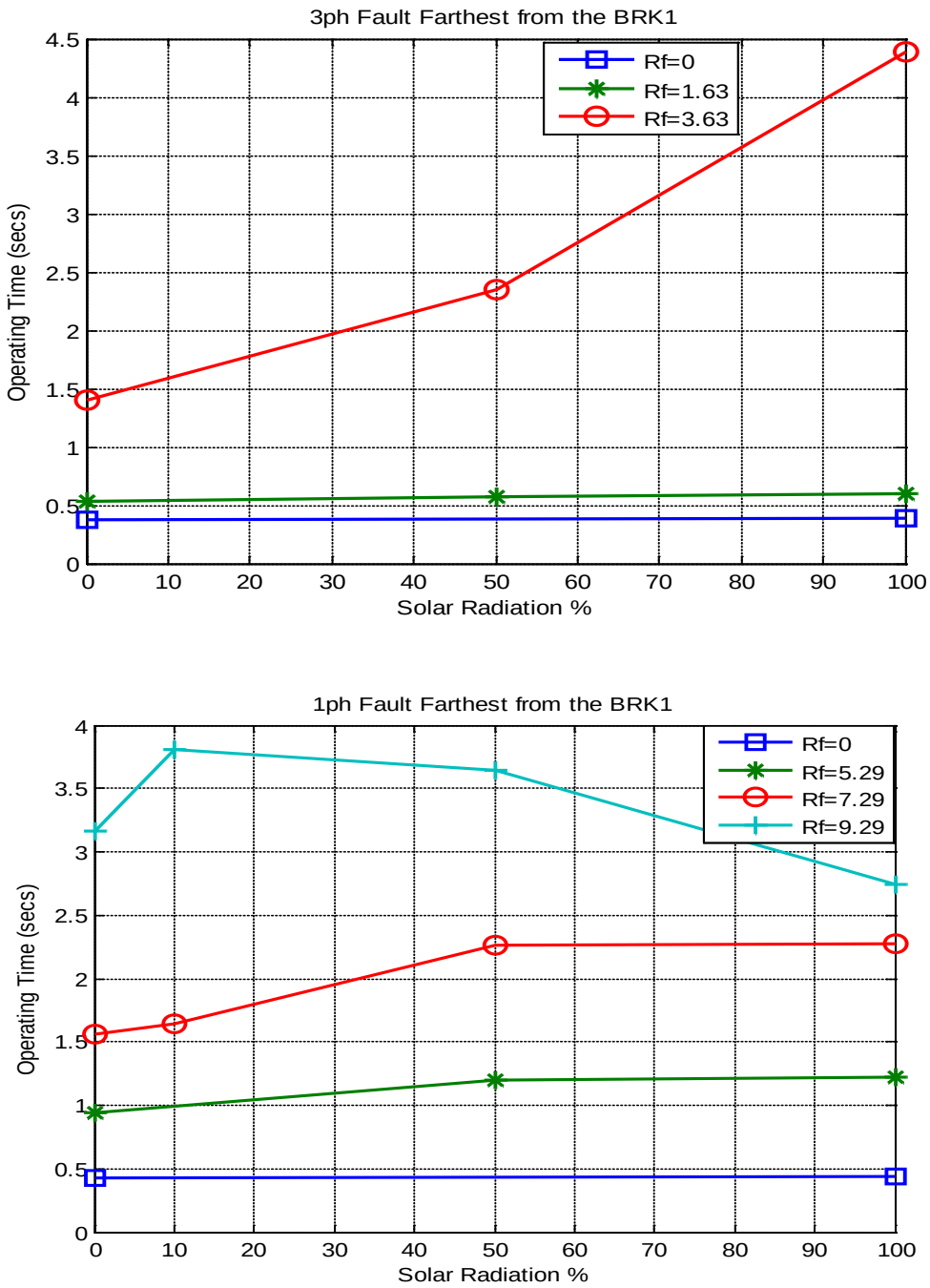

Figure 27 Breaker Op. Time vs. PV generation for faults on the End of Feeder

Similar plots from PSCAD simulations taken from [1] are shown below in Figure 28.

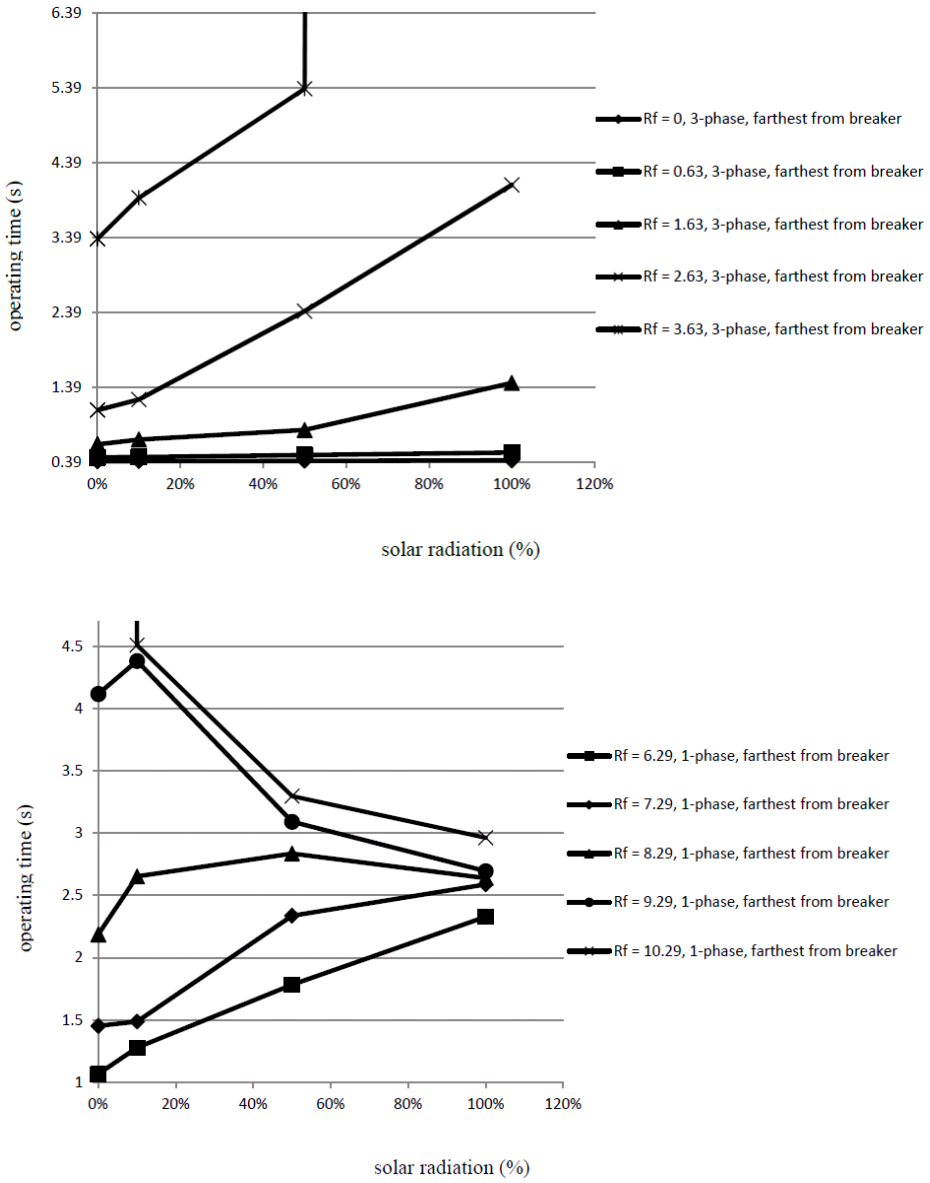

Figure 28 Breaker Op. Time vs. PV generation for faults on the End of Feeder in PSCAD [1]

Except for the case Rf=3.63Ω in Figure 27, all of the results closely match which reiterates the accuracy of our HIL test bed. For instance, in Figure 27 consider the 3ph fault case for Rf=1.63Ω and 50% solar radiation, HIL relays operated at 0.6 sec approximately and the PSCAD at 0.5 sec as seen in Figure 28. It is seen from the figures that increase in PV's generation increases the operating time of the phase relay for distant faults. The pattern is more pronounced with the increase in fault resistance. In the case of single phase distant faults, since all the PVs are present downstream of the relay as seen in Figure 4; increase in PV generation improves the operating time at higher fault resistances as shown in .

2. Breaker Close-in faults

Figure 29 summarizes the effect of PVs on the operating of the breaker for close in faults on the main feeder.

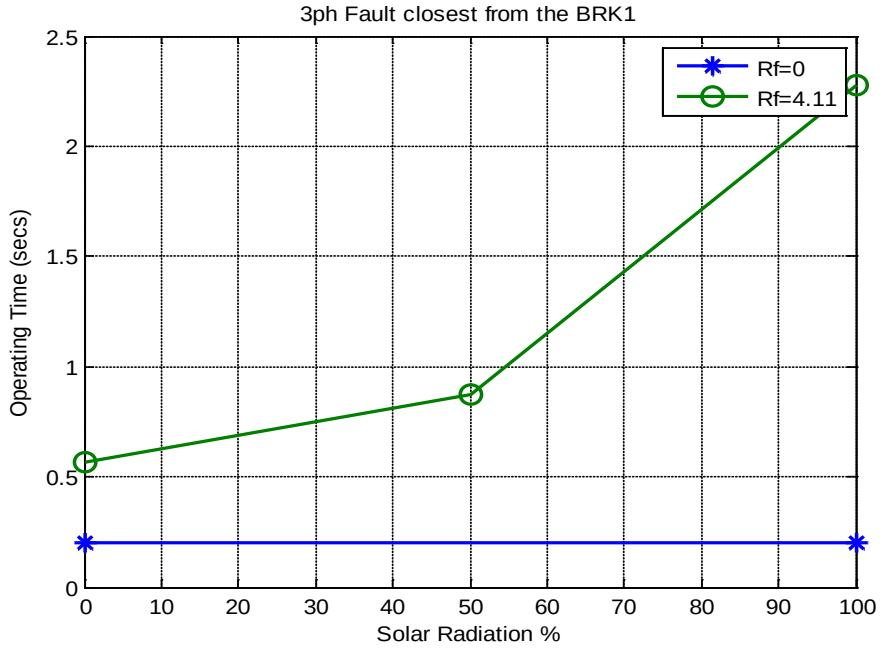

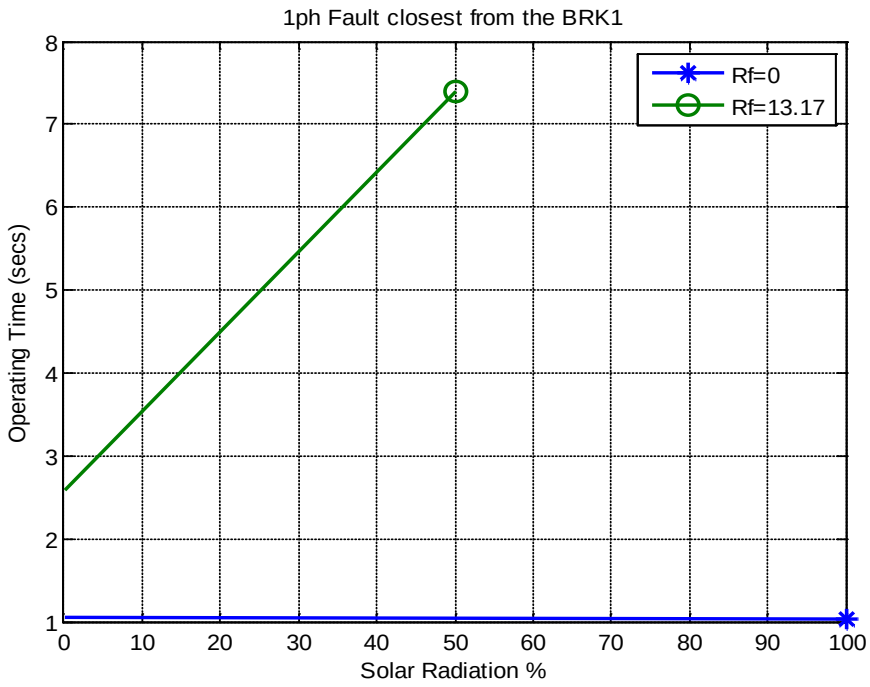

Figure 29 Breaker Op. Time vs. PV generation for close in faults

In Figure 29 it can be seen that 1 ph close-in faults have considerable impact on the ground relays. With all the PVs downstream of the BRK relay, a high impedance fault of Rf=10.75Ω triggers the relay to operate at 7 sec approximately even for a 50% of the PV load contribution.

3. Recloser Distant Faults

Figure 30 shows the impact of PVs on the operation of the recloser (RCL) for distant faults on the main feeder. In the case of distant faults for RCL, 3ph faults have the same impact as an in BRK; increase in PV generation increases the operating time of the RCL relay. But in the case of 1ph faults, since the upstream PVs' contribution to the fault current is more than

the downstream PVs in the case of RCL, it's seen that the increase in solar radiation for a 1ph fault improves the operating time of the relay at higher Rf (Rf=10.75 in Figure 30).

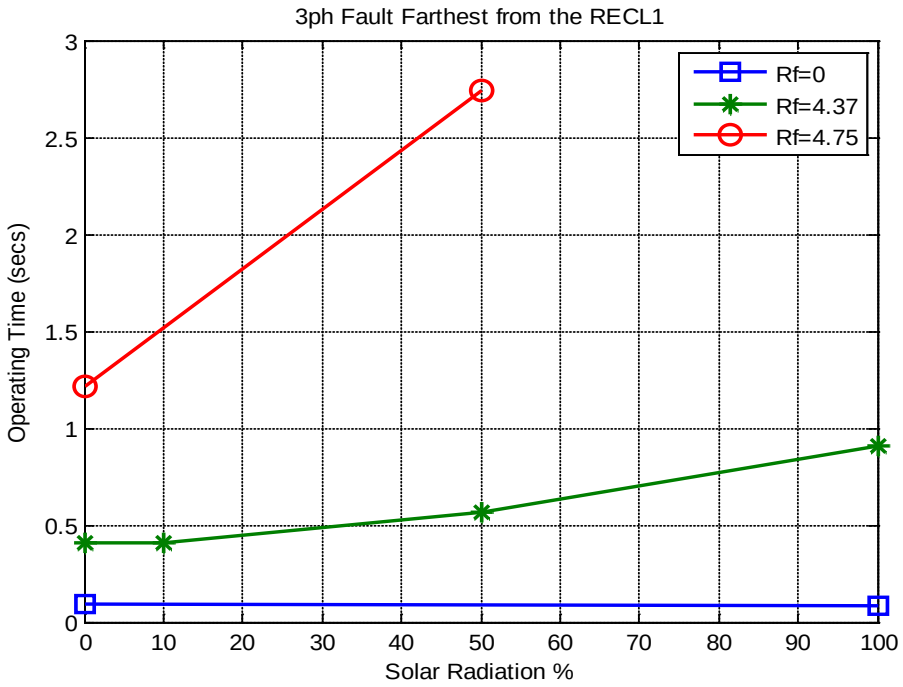

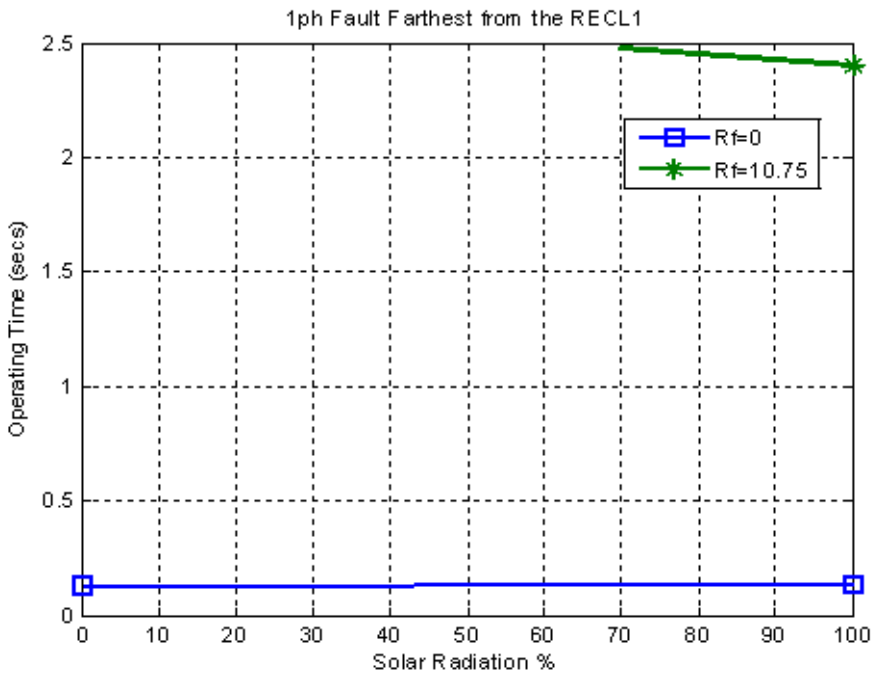

Figure 30 Recloser Op. Time vs. PV generation for faults on the End of Feeder

4. Recloser Close-in Faults

Figure 31 shows the impact of PVs on the operation of the recloser for close-in faults on the main feeder. The close-in 3ph faults have the same impact as the distant 3ph faults. In the case of 1ph faults it can be seen that the impact is more pronounced, causing the relay to operate with a higher delay. Due to presence of upstream PVs for RCL both in distant and close-in 1ph faults, the increase in PV generation only improves the operating time of the relay. The patter is more pronounced with the higher fault resistances.

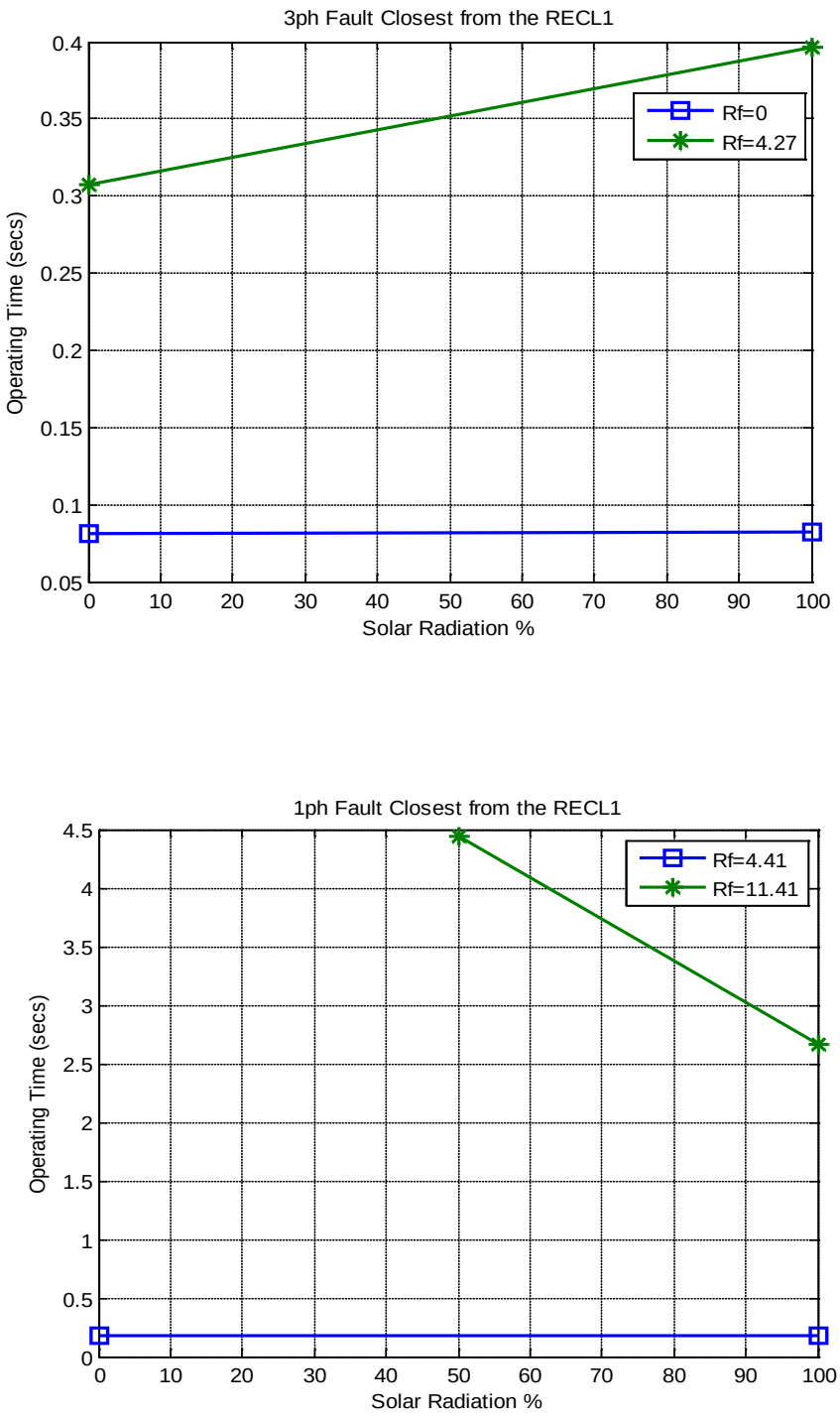

Figure 31 Recloser Op. Time vs. PV generation for close in faults

The above discussed cases verify the impact of PVs on the performance of the relay operation and support the claims made in chapter 1. The comparison of PSCAD results from [1] with the HIL system shows that the presence of PVs affects the operation of the relays in the same manner in both.

On the whole, the following insights can be gained from these results:

- 3 Phase faults: Irrespective of PVs' location, it is seen that increase in the generation of PVs increases the operating time of the relays. This means both the reach and speed of the relays are reduced.
- 1 Phase faults: If more PVs are present downstream of a protection relay, close in faults reduces the reach and speed of the relays. For end of feeder faults the PV generation actually increases the reach.

The worst case scenario due to PV generation occurs when:

3 Phase faults:

- Amount of PV generation: 100%
- PVs Location: Downstream from the relay
- Fault Resistance: Maximum (the fault resistance for which the fault current equals the relay pick up current)
- Fault Location: At the End of Feeder (Distant faults).

1 Phase faults:

- Amount of PV generation: 100%
- PVs Location: Downstream from the relay
- Fault Resistance: Maximum (the fault resistance for which the fault current equals the relay pick up current)
- Fault Location: At the beginning of feeder (close in faults).

3.2 Loss of Coordination

We have seen that the presence of downstream PVs reduces the current seen by the protective relays and thereby increases its operating time. This can cause loss of coordination between the downstream devices. This issue has been identified and investigated by Dr. Hossein in [1]. In the HIL study some of the simulations from [1] has been repeated. Figure 32 depicts the test case in which the relay (PD1) has all the DGs downstream to it and PD2 has on both its sides. By creating a fault at the shown location, the coordination of the relay can be tested at the minimum margin.

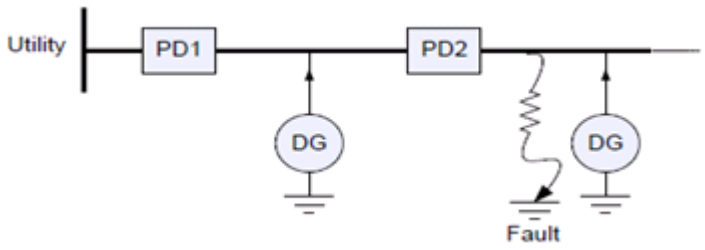

Figure 32 Loss of Coordination in the presence of a DER

It is known that the coordination margin is least between two downstream devices for maximum fault current. The maximum fault occurs just ahead of a downstream device. Figure 33 shows the coordination margin between the BRK and RCL relays of the HIL system.

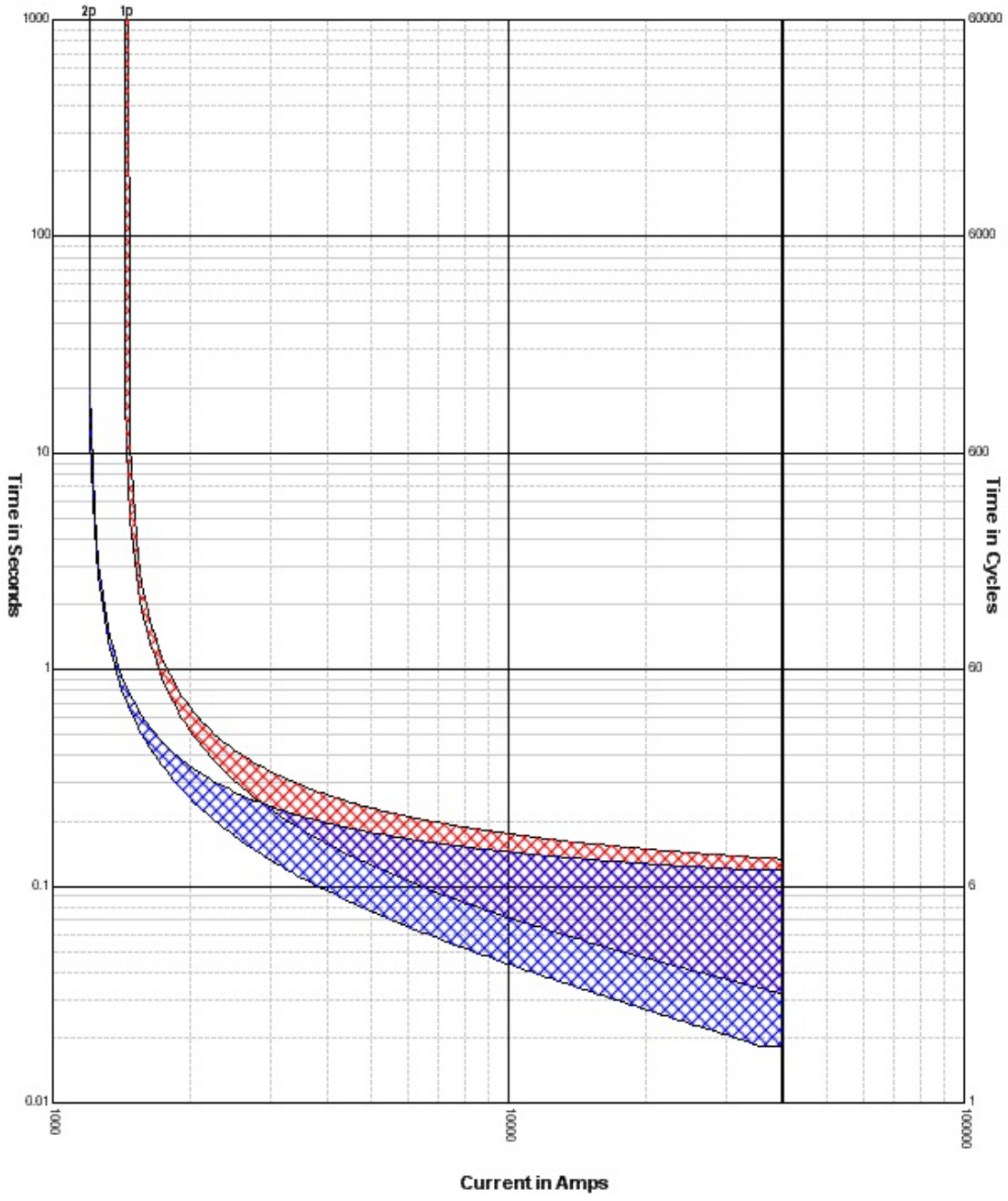

Figure 33 Time coordination curves for the Breaker (Red) and Downstream Recloser (Blue)

3.2.1 Test Results

In the system, the worst case scenario could be for a 3ph fault right after the RCL (at F2 from Figure 26) with all the PV's present downstream to the BRK. In this condition, fault current seen by the PD2 is the maximum and appears in the area where the coordination time between the protective devices is the least as seen in Figure 33. PVs downstream of BRK do not have an effect on the fault as compared to the current contributed from the substation transformer. This is because the substation's contribution to the fault current is much higher than that of the PVs. Thus PVs do not affect the coordination between downstream devices. However their impact on high resistance faults is a topic of interest for investigation.

Figure 34 shows the operating time margin between the breaker and recloser for a 3ph phase fault condition. A bolted fault located right after the recloser was applied for this case. As seen in the Figure 34 the operating margin is not affected by the PVs at all.

Figure 35 shows the operating time margin between the breaker and the recloser for high resistance fault of Rf=4.41Ω. The presence of downstream PVs only reduces the fault current seen by the breaker relay. This helps in increasing the grading margin between the breaker and the recloser relays due its inverse time characteristics. In this case it is seen that the margin increases from 0.9 sec with 0% solar insolation on PVs to 3secs for 100% PVs' solar insolation.

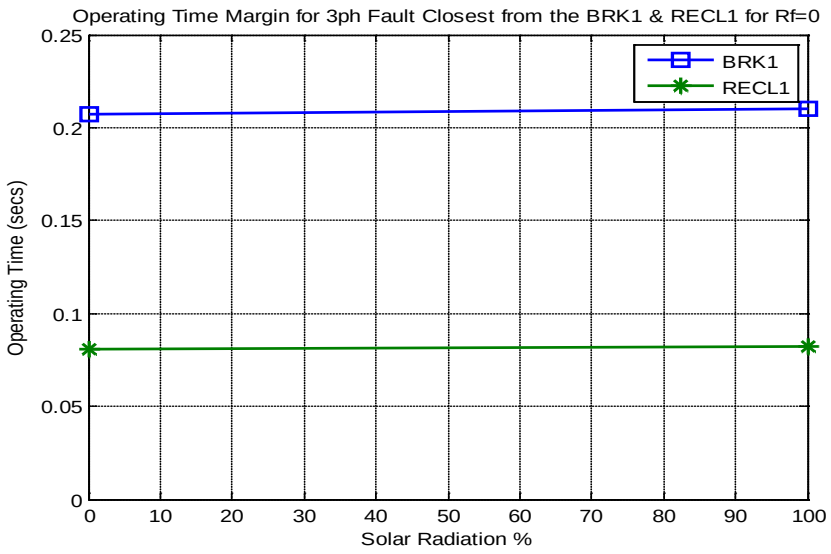

Figure 34 Marginal time between the operating times of the breaker and the recloser 3ph fault with Rf=0.

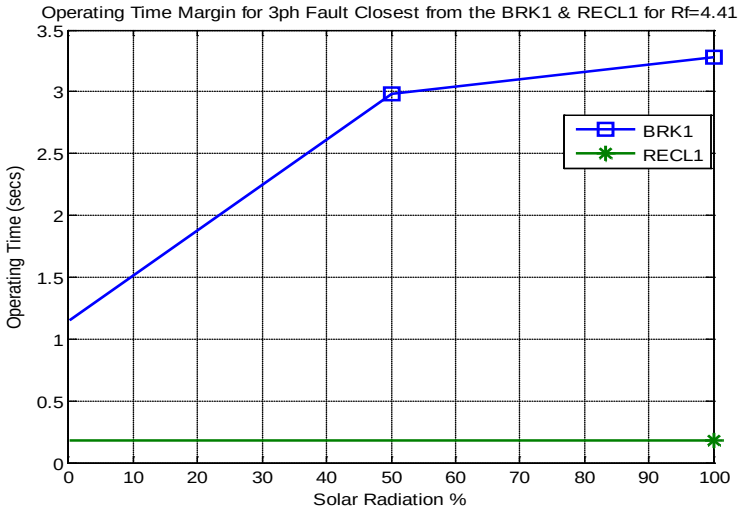

Figure 35 Marginal time between the operating times of the breaker and the recloser for 3ph fault with Rf=4.27.

The PSCAD result for the same test case is shown below in Figure 36. The operating margin in this case was 2.498 sec for a 100% solar radiation. In the HIL system the same was measured to be 3.3 sec.

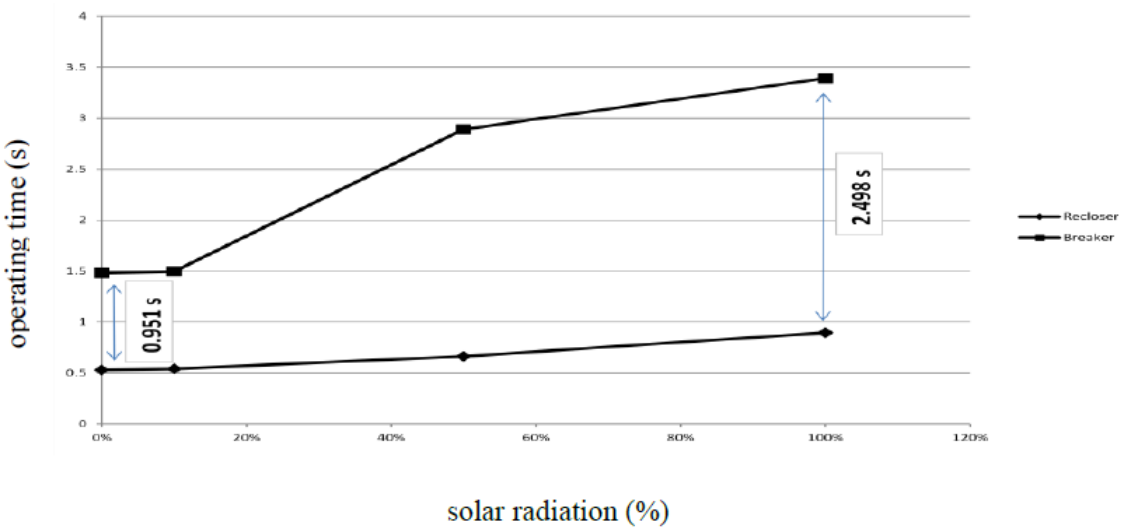

Figure 36 Marginal time between the operating times of the breaker and the recloserfor 3ph fault with Rf=4.27 from PSCAD [1].

Thus using the HIL system we have proved that PVs do not impact the grading margin between downstream relays.

Chapter 4: Mitigation of Protection Issues in Green Energy Hub

In Chapter 3, we investigated the protection issues pertaining to the presence of PVs in the distribution feeder on the HIL test bed. It was proved that the presence of PVs downstream to a protective relay reduces the reach of the relay and increases its operating time. To mitigate this impact, a set of guidelines was previously proposed by Dr. Hossein in [1]. In this chapter we repeat these guidelines in the HIL test bed to verify the effectiveness of this solution. By doing so we should be able to restore the relays' original reach in the absence of PVs.

4.1 Procedure:

Hossein claimed in [1] that mitigation of protection issues can be achieved by changing the existing settings in the relay itself. The procedure he had used to set the relay models in PSCAD is explained here. As per the traditional guidelines the initial pick up current for the relay is set higher than twice the normal current but less than one third of the minimum fault current that flows through the protective device. The minimum fault current for a particular relay is obtained by applying a bolted fault to the end of of its reach without the presence of PVs. In Chapter 3, we had found the maximum fault resistance (Rf) for which the existing settings in the relay picks up. The goal of this new scheme is to modify the relay settings so as to compensate for the current seen by the relay for the Rfmax in the presence of PVs and thereby take care of the reduction in reach and speed problem induced. In other words, the current seen by the PD with the presence of PVs for the identified Rfmax is determined and used as the new pickup value. The procedure to be followed is listed below:

- Identify the minimum fault current that can be seen by the relay with the existing settings.
- Identify the Rfmax for each relay.
    - For the Phase relays, Rfmax is to be calculated by injecting the fault at the end of the feeder as the effect of PV is greatest when the fault is far away from the PD.

- For ground relays the fault was injected at the start of the feeder since the effect of PV is greatest when the fault is close to the PD.

- If the current seen by the relay at Rfmax is less than the minimum fault current identified before, then replace the pickup settings to this current. To maintain coordination, measure the current for Rfmax of the downstream relay too. Choose the pickup for both the PDs to be the minimum of these two values.

4.2 Test Results

Based on the proposed scheme, both the BRK and RCL relay settings have been modified in our HIL system. The procedure followed is explained below:

Phase Relays: The most downstream relay being the recloser, the pickup current for this relay is calculated first. The original setting was 1245A and the corresponding Rfmax was 4.75Ω located at the end of feeder. In RSCAD, the current seen by the recloser in the presence of PVs for this Rfmax was 1138A which is more than twice the feeder nominal current. For the beaker relay, the original settings were 1460A and the corresponding Rfmax was 4.15 located at the end of the branch just before the recloser. The current seen by the breaker in the presence of PVs for this Rfmax was 1111.8A which is also greater than twice the nominal current. Since this current is lesser than that seen by the recloser both these devices are set at 1112A. The time dial of the breaker relay has been changed from 0.36 to 0.48 to maintain the grading margin with the recloser. Based on these changes, the operating time of both the breaker and the recloser relay has been shown along with the old settings in Figure 37.

In the case of breaker, at 4.75Ω (Rfmax), the modified settings gave us an improved operating time of 2.5 sec approx. which is far better than the old settings of 4.5 sec. Similarly in the case of Recloser at Rfmax of 4.15, a far better improvement is seen than its older settings.

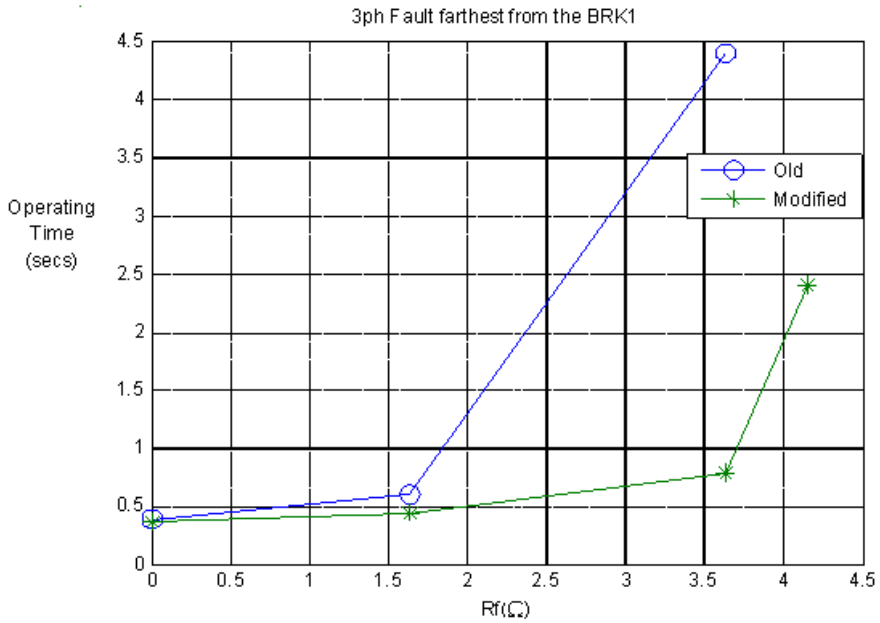

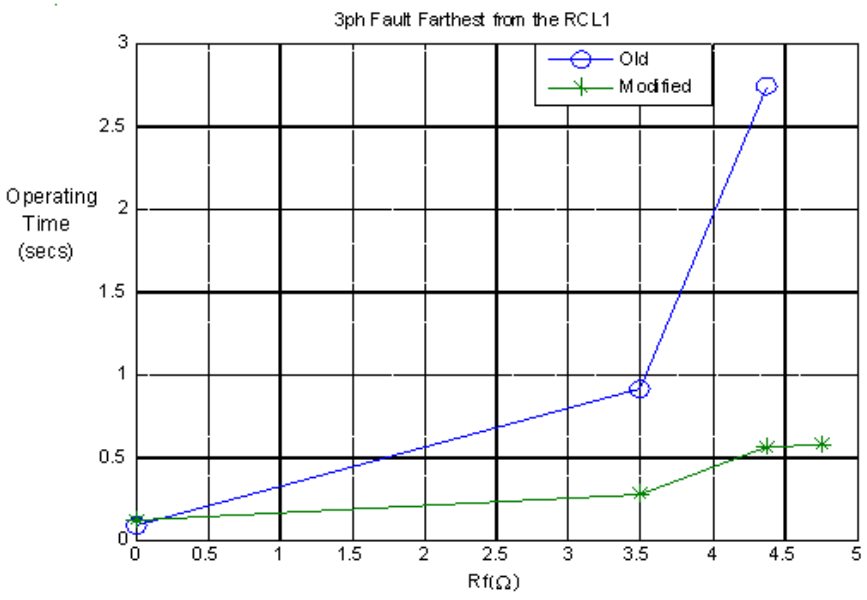

Figure 37 Operating time of phase relays for BRK & RCL with the modified settings

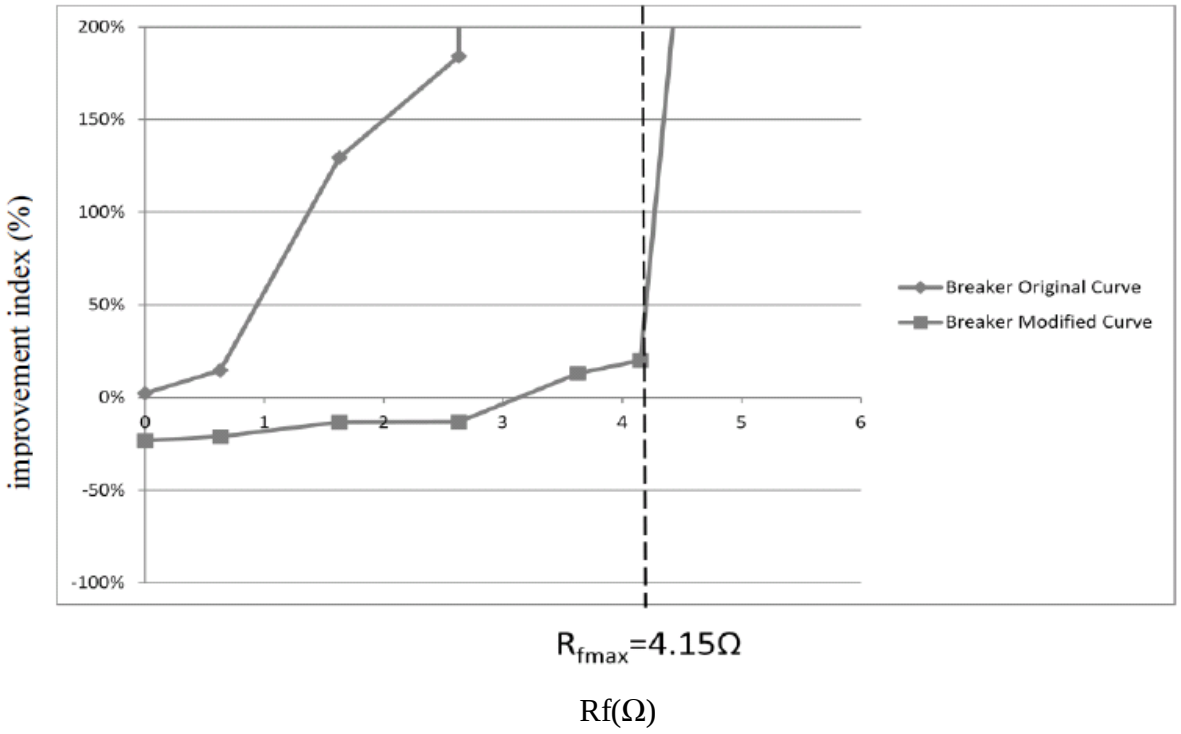

Figure 38 PSCAD BRK Relay- Improvement with modified settings [1]

Figure 38 shows the improvement index of the breaker relay in PSCAD from [1]. At Rfmax=4.15, the index shows a 20% improvement in reach. The same when measured for the relays was 35% as calculated from Figure 37.

Ground Relays: In the case of ground relays, close in faults had the maximum impact on the settings. Therefore the resistance Rfbmax needs to be determined for close in faults beyond which the relay doesn't pick-up for the fault in the presence of PVs. The original settings for the recloser was 480A and for a close in fault at a maximum resistance of 2.1Ω still gave a fault current of 520A which meant no changes required for the recloser settings.

The original setting for breaker was 480A; the close-in maximum fault resistance was 15.3Ω at the beginning of the feeder. For this condition the fault current seen by the breaker was 405A which was below the pickup value (480A). For the new pickup current 420A was chosen considering the value to be more than the maximum unbalance in current when one of the phases was disconnected (400A). For the sake of maintaining the gradation between the two devices the new time dial settings was chosen as 1.4 for recloser and 2 for breaker. Figure 39 shows the performance characteristics of the protection devices for both the old and new settings.

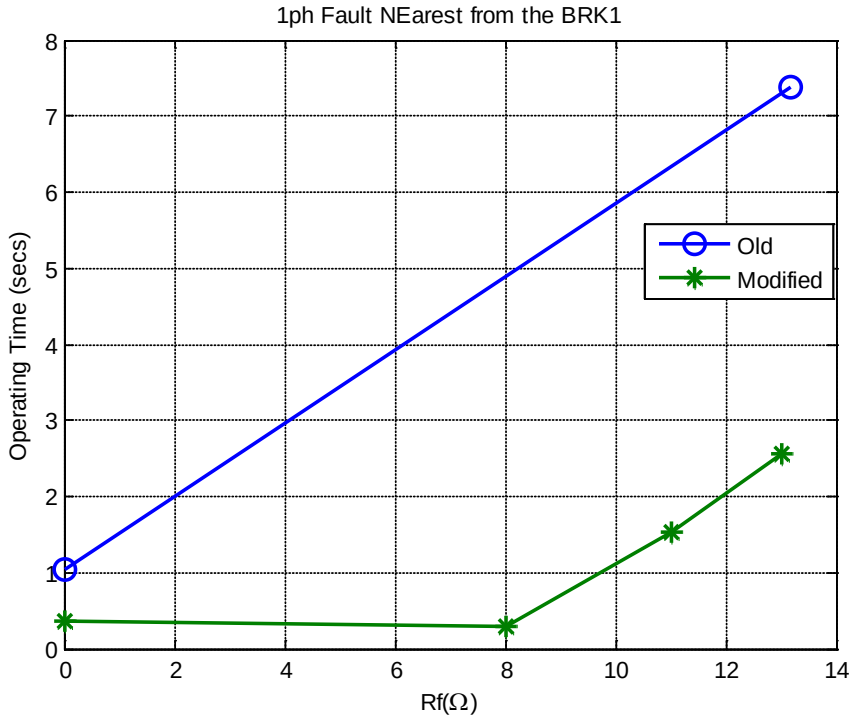

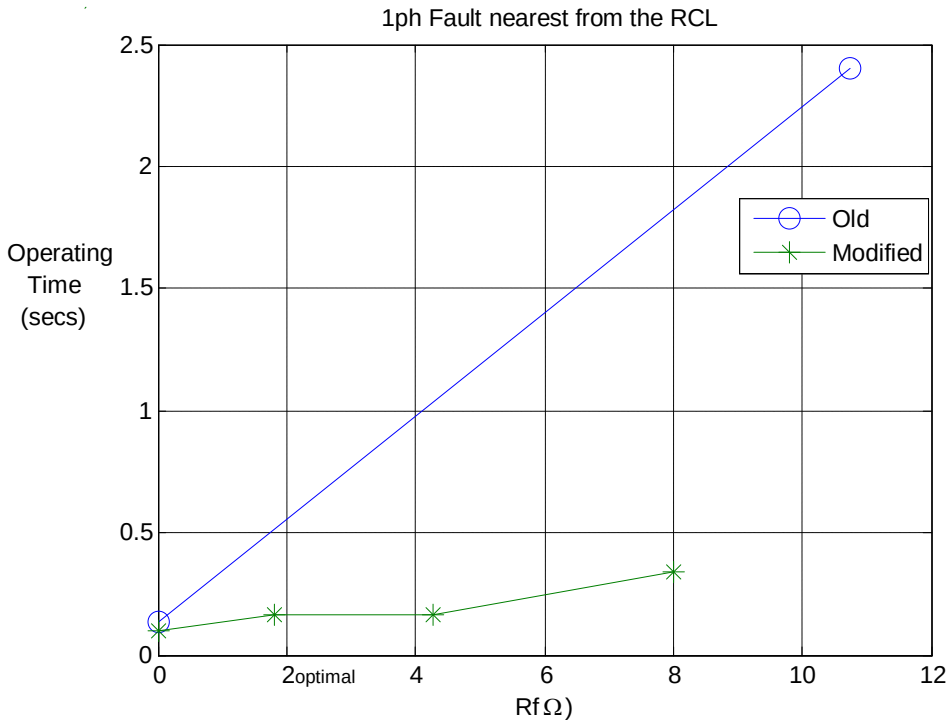

Figure 39 Operating time of ground relays for BRK & RCL with the modified settings

These results confirm that the modified relay settings have extended the relays' reach in the presence of PVs for both the breaker and the recloser; also the operating time of these relays have been significantly improved. Therefore the modified settings have helped in mitigating the problems imposed by the PVs distribution feeder protection relays.

Chapter 5: Coordination between Protection Relays and Fuse

In the previous chapters, we had considered the impact of PVs on protection relays only. Various cases were analyzed to study the problems caused by PVs on the operation of protective relays. We had also checked impact on the coordination of relays by the presence of PVs. But in an actual feeder there even exist the fuses downstream of protective relays. Hence there arises the need to check the coordination the relays with these fuses.

5.1 Recloser Fuse Coordination

In chapter 4 to compensate the effect of PVs on the operation of relays, the pickup current of the recloser was reduced. By doing so, the relays have become more sensitive and respond quicker. To study the impact of this setting over the fuse operation, two fuses of S&C make 200T and 100T are placed on the lateral at line section Ln 5 and Ln 9 of the RSCAD simulation system as shown in Figure 40. 200T being the slowest of the two, it's located at the start of the lateral. PV's are distributed accordingly based on the load distribution on the lateral. Fig 39 gives a clear picture of the location of the fuses and the location of PVs on the lateral.

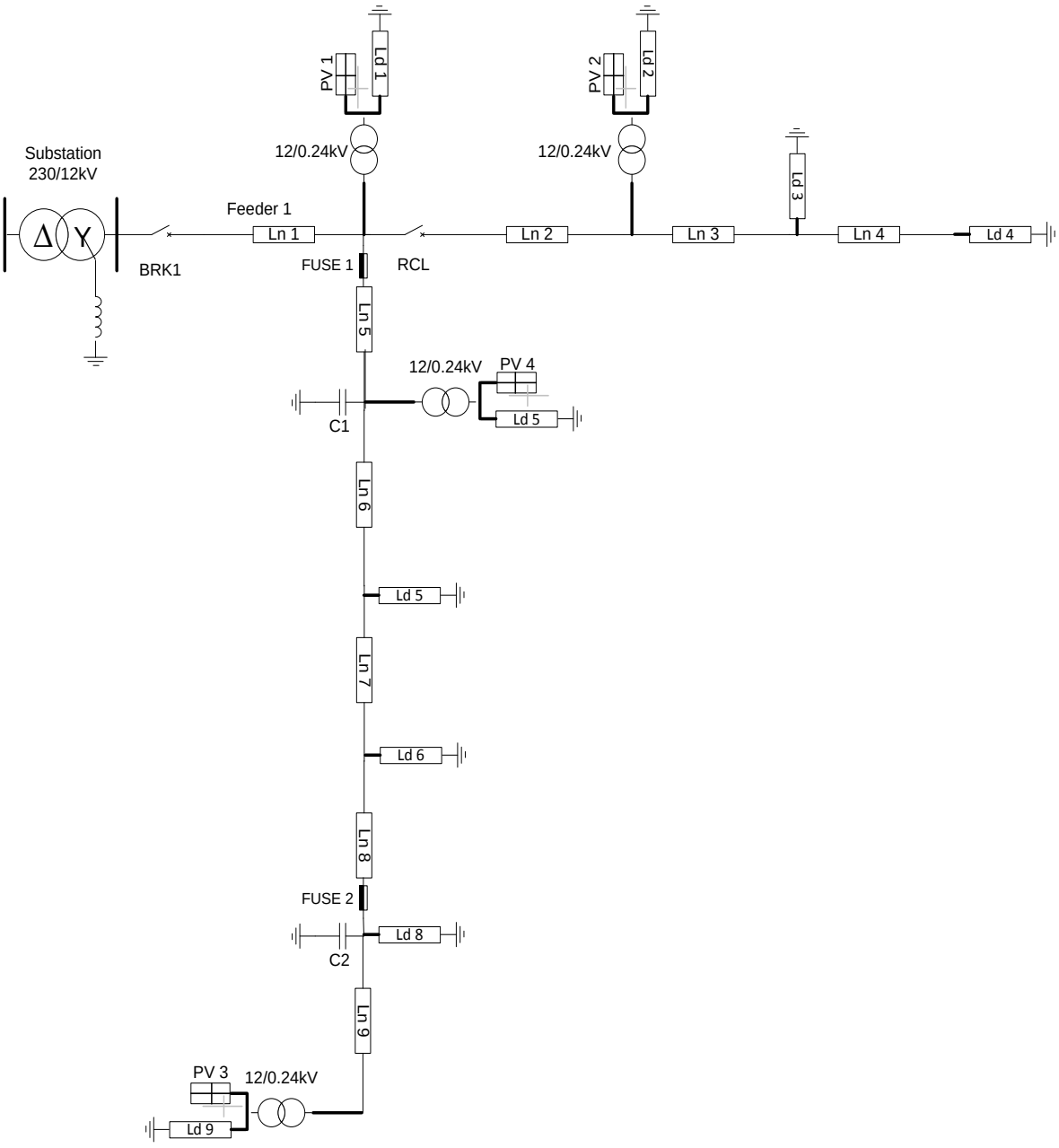

Figure 40 FREEDM Green Energy Hub with fuses

In the GEH system, the fuses are coordinated after the fast curve of the recloser relay curves. Upon first operation of the relay fast curve, if the fault still persists the fuse is allowed to blow. The slow second curve is stacked right above the fuse curve. Figure 41 shows zoomed in version of the recloser curves coordinated with the 200T fuse. Therefore the coordination of fuses needs to be checked only with the slow curve of the relay.

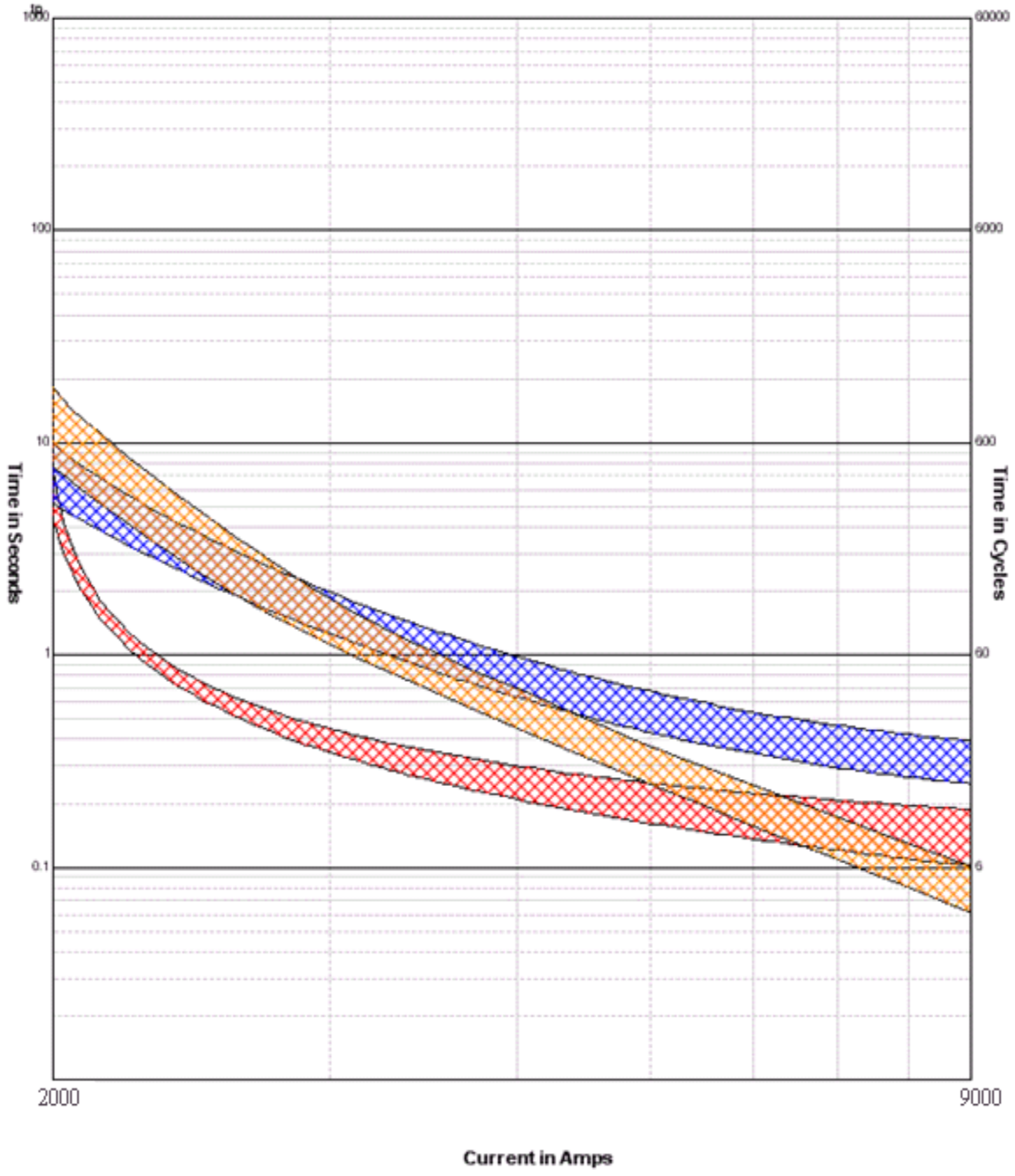

Figure 41 200T Fuse (orange) coordination with the recloser Relay curves (red and blue)

As seen in Figure 41, the coordination is not perfect throughout, but within the system fault current range of 2200A to 7000A, the recloser curves (red and blue) and fuse curve (orange) is stacked appropriately. We do know from the previous chapters that the presence of PVs' reduces the fault current seen by the protective devices, and this impact is predominant on high impedance faults. Thus the presence of PVs may introduce a loss of coordination between the fuse and the recloser's slow curve which is studied in this chapter.

5.1.1 Fuse Model in RTDS:

The fuses have been implemented as breakers with overcurrent protection in RTDS. The actual system had two fuses on the lateral.

The relay curve equivalents for the fuses have been identified as follows:

- For 200T – ABB DPU 2000R IEC Extremely Inverse Curve, Pickup-600A, Time Dial-0.15.
- For 100T – ABB DPU 2000R ANSI Extremely Inverse Curve, Pickup-200A, Time Dial-3.72.

Figure 42 shows the equivalent curves along with the original curves.

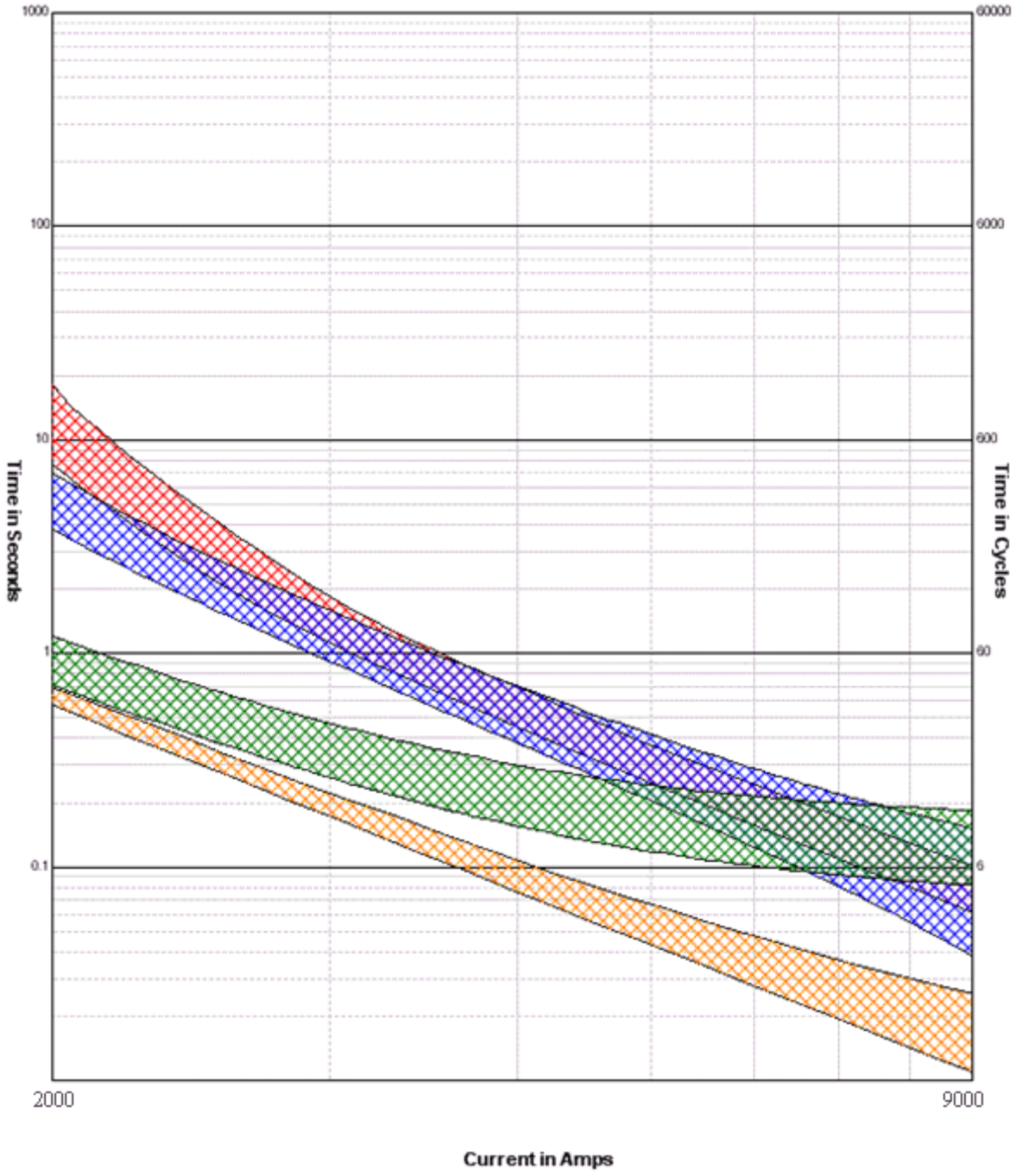

Figure 42 Fuse Curve Equivalents for 200T (blue) and 100T (green)

It can be seen that for the fault current of our system which is between the 2200A and 7000A range the curve fit provides enough operating margin between the fuse models. This was the basis for the selection of these curves.

5.1.2 Test Results:

In order to identify the potential problems introduced by PVs in the protection system that included fuse, tests were conducted on the RSCAD simulation platform. The goal was to find that maximum fault resistance for which the relay slow curve tripped along with the fuse. This is a potential loss of coordination problem. In this study we have included the impact of PVs' on the fuse operation for various fault resistance and eventually have determined the critical Rf for which the loss of coordination condition occurs. A 3 phase fault was created at the end of the feeder just before the 100T fuse with various fault resistances. The recloser was loaded with the slow curve; with the settings SEL U3 curve with pickup 720A and time dial 2.3.

Before conducting the test cases for loss of coordination problem, the impact of PVs on the operation of the fuse was studied Figure 43 shows the operating time of 200T fuse for various Rfs. The PVs' output has been varied by changing the solar insolation between 0 to 100%.

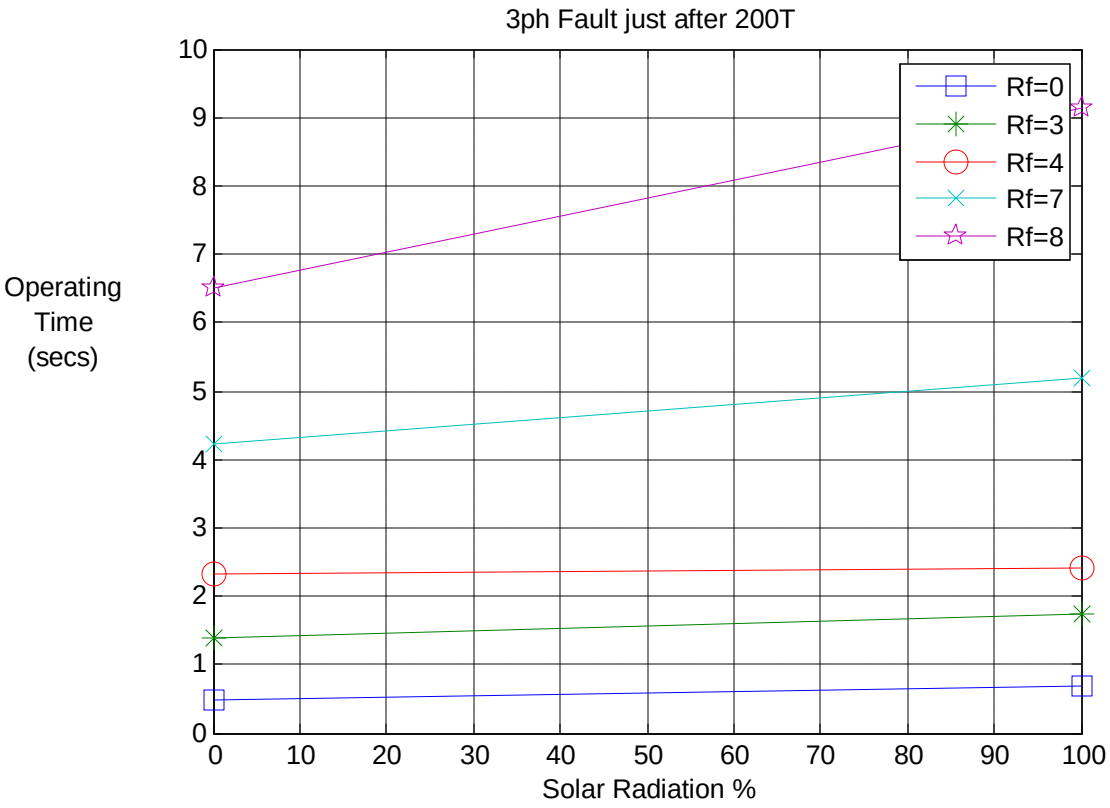

Figure 43 200T Fuse Op. Time vs. PV generation for faults on the End of Feeder just before the 100T fuse.

It's seen in Figure 43 that the presence of PVs increases the operating time of the fuses. Also with the increase in Rf, the impact is predominant.

For the loss of coordination test case, it was noted that for Rf=4Ω the fault current seen by the fuse was 1248A. for this Rf, at 100% solar insolation, the 200T fuse and the recloser operated almost together. Beyond this since the current seen by the fuse reduces to the region where the curves overlap, the loss of coordination issue occurs.

Figure 44 shows the impact on fuses and recloser coordination. A 3ph fault was created right at the terminals of the 200T fuse for various fault resistances. It can be seen that at Rf=4Ω the operating time for both the recloser and the fuse are almost the same. Beyond this the fuse trips after the recloser which is a clear loss of coordination.

It is to be noted that the difference between the previous test case and this case is that the location of the fault is changed. As such in both cases since the distance was not much different, the difference in fault current was very minimal as seen by both the fuse and the breaker.

Potentially anything beyond Rf=4Ω caused a loss in coordination between the relay and the fuse.

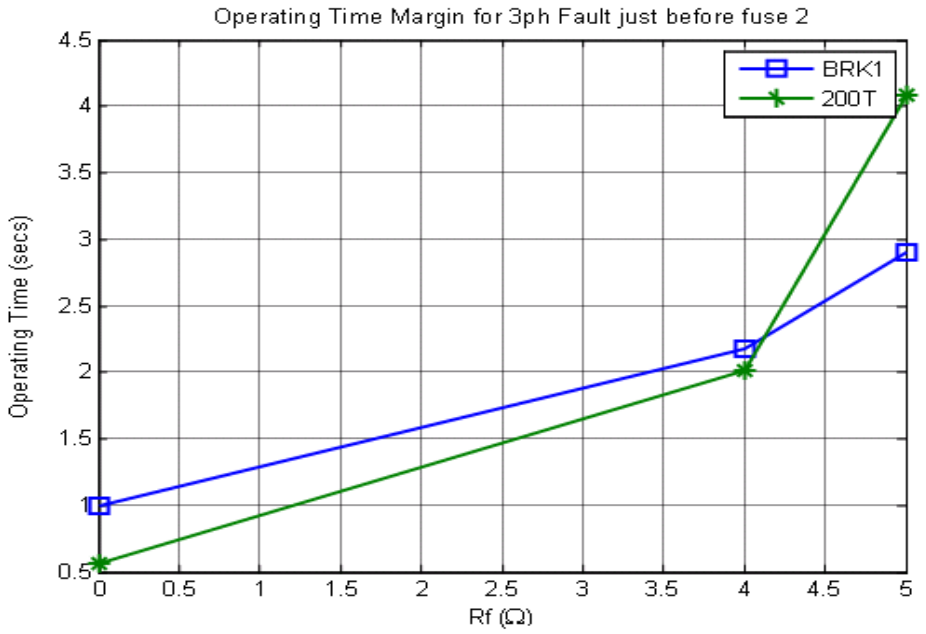

Figure 44 Coordination issue with Breaker Relay and the 200T fuse.

Figure 45 shows the operating curves of the breaker relay and the fuse curve. The fault currents seen by the breaker for various fault resistances are shown as vertical lines(I1,I2 & I3) It can be seen that for Rf=4, the fault current seen by the breaker (I1) appears in the region where both the fuse and breaker's slow curve merge. Hence there occurs an in-coordination between the two devices. In the same curve the fault current seen by the breaker in the absence of PVs is also shown at I3, this time the coordination is still maintained between the devices, since the fault current is far away from the lack-of-coordination region.

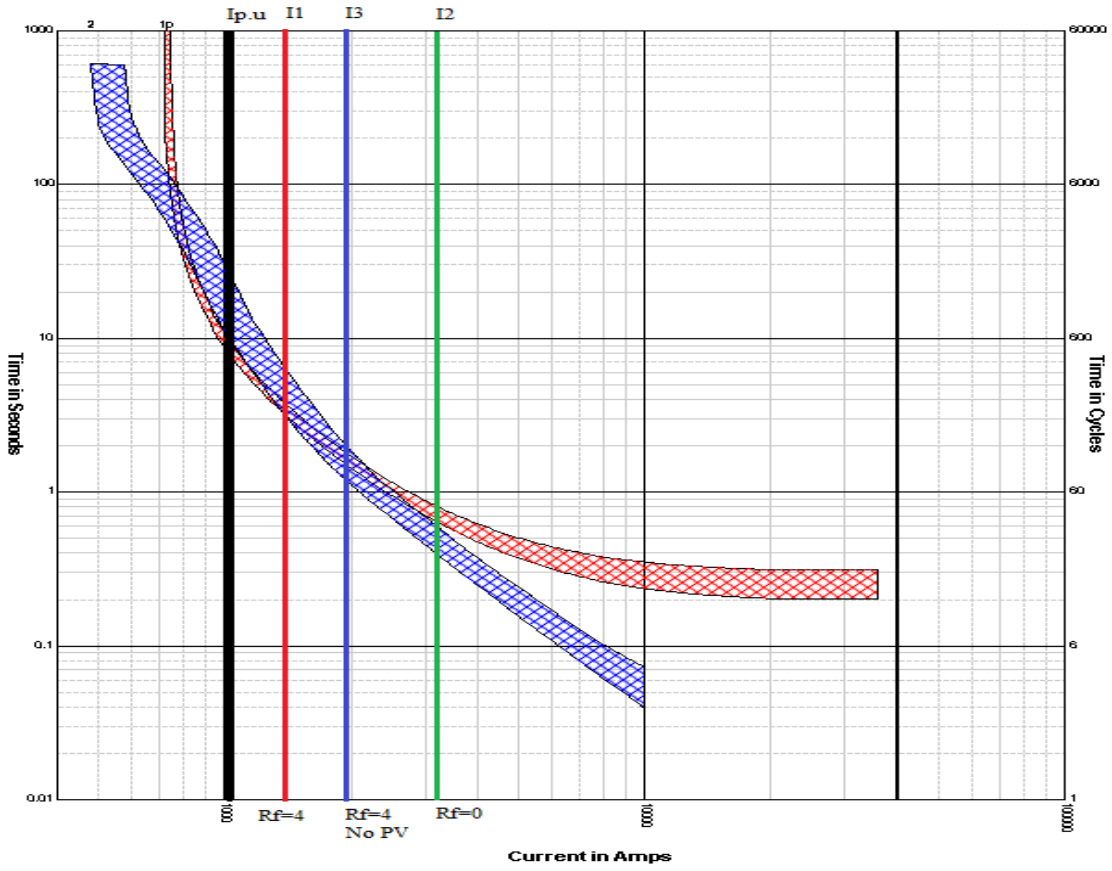

Figure 45 Fault currents on the operating curves of the Protection devices

5.2 Coordination between 200T and 100T Fuses

The 200T and 100T fuses are stacked in such a way that they do not introduce any additional loss of coordination in the protection scheme. Since the fuses also have inverse time current characteristics, the presence of PVs' which apparently reduces the fault current seen by these devices do not cause any loss of coordination. Also when stacked with the breaker slow as shown in Figure 46 the 100T fuse is well coordinated with the recloser. So at high fault resistances in the presence of PVs', though the fault current reduces significantly, the coordination of 100T fuse with 200T fuse or the recloser relay slow curve is not affected.

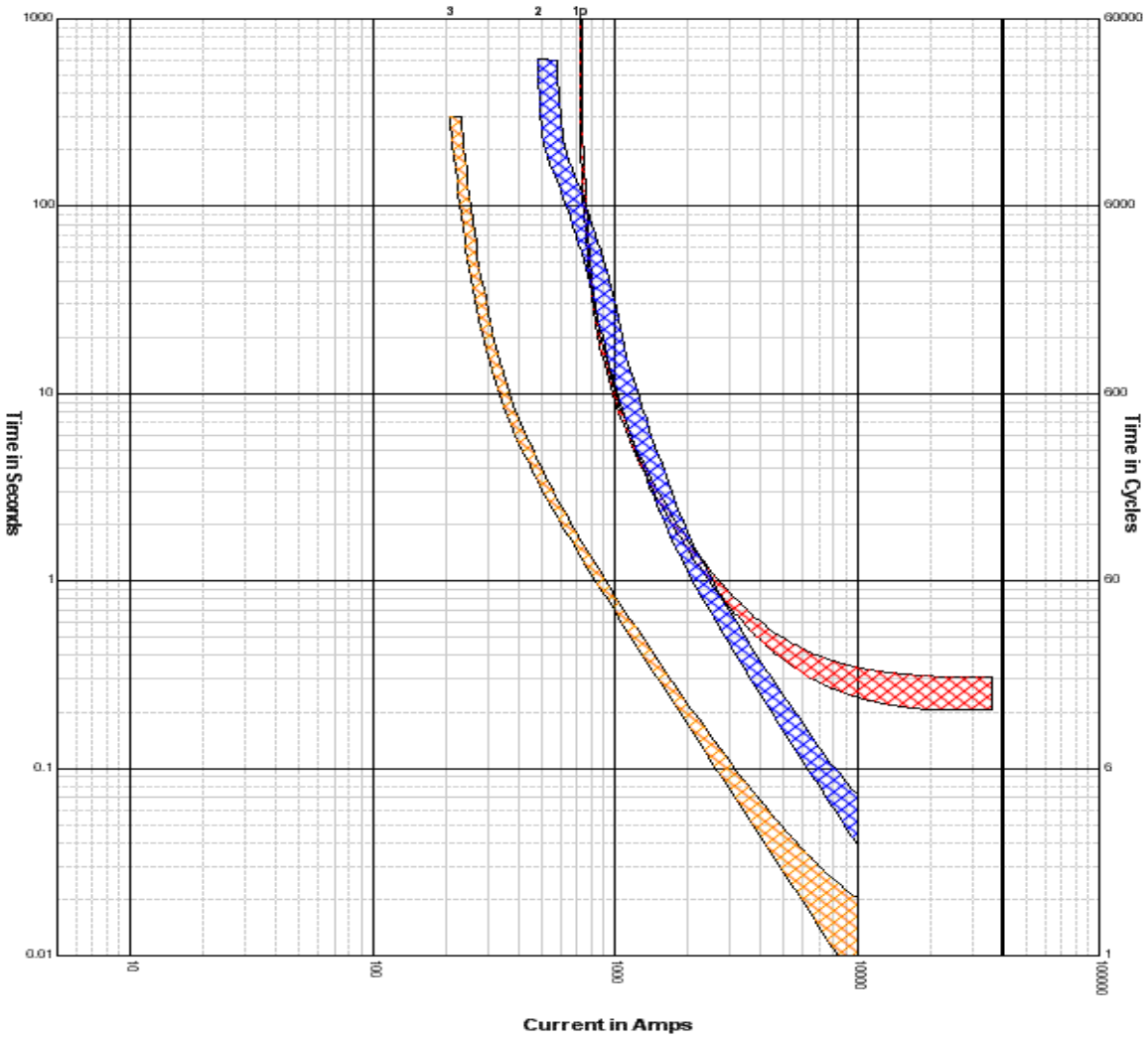

Figure 46 Inverse time characteristics of Recloser Relay slow curve (red), 200T (blue) and 100T (orange) fuses.

5.2.1 Test Results

To better understand the coordination margin available between the two fuses RSCAD simulations were done by introducing a fault right at the terminals of the 100T fuse and the operating time of both the 200T and 100T were calculated for various fault resistances.

Fig 47 shows the operating margin available between the two fuses. Clearly in consonance with the curve characteristics, higher impedance faults only improve the coordination between the fuses. But one thing has to be noted that even in this condition for higher impedances the loss of coordination occurs between the relay and the 200T fuse.

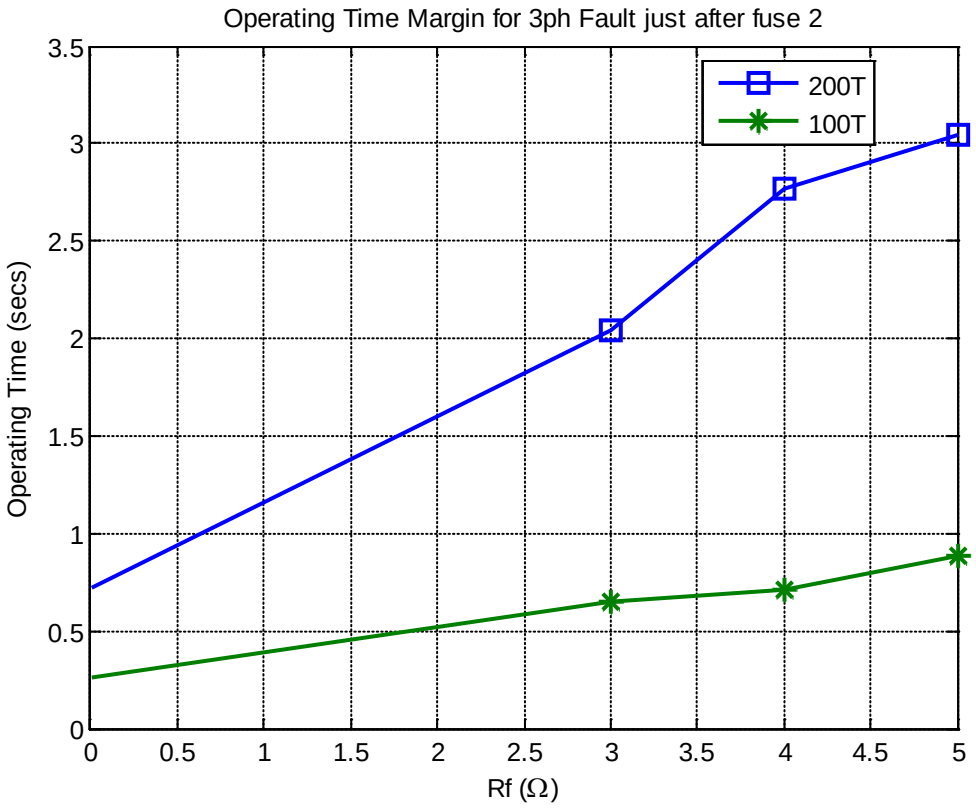

Figure 47 Op. time Coordination between 100T and the 200T fuse.

Based on the results shown in this chapter we can conclude on these following insights:

- The presence of PV's increases the operating time of the fuse. Because of this for high impedance faults the coordination between the fuse and the upstream relay is affected. As a result simultaneous or improper tripping of both the breaker and fuse may occur.
- The worst case condition for the loss of coordination issue is when the fault is located right at the end of feeder just before the downstream fuse.
- The coordination between downstream fuses is not affected by the presence of PVs.

Chapter 6: CONCLUSIONS

The major portion of this thesis is devoted to comparing the simulated results from Dr. Hossein's thesis with the Hardware in the loop system built using the RTDS. In chapter 2 of this thesis, the HIL test bed was introduced and the basic verification of this test bed was performed. The purpose of this verification was to establish that the HIL system indeed resembled the simulated system. In fact, the RTDS only emulated a more realistic environment with actual relays present. A new model of the PV specifically designed for the RTDS application was also introduced.

In chapter 3 all the problems highlighted in [1] with regard to PVs present downstream of a protective relay were analyzed and the test results were compared with the PSCAD simulations. In chapter 4 the guidelines provided in [1] to mitigate the effect of PVs on the operation of the protection devices, were administered. The results of the test confirmed the validity of these recommendations. In chapter 5, we identified the possible cases where fuses in the system affect the existing coordination of protective devices. Tests carried out on the RSCAD simulation platform confirmed that in such cases, there was a loss of co-ordination between upstream protection devices and the fuses. This is despite the application of the recommendations in chapter 4. Additionally, we were able to test the accuracy of relay models on the RSCAD platform by comparing their performance with that of the actual relays.

A simulation-only environment would be suitable for a system study at a macro level and can help identify any possible implications. However to study the possibility of overcoming these problems, the effects of implementing new technology, or to validate the performance of a particular device, a micro level analysis that utilizes HIL becomes imperative. Thus, while the recommendations as provided in [1] can also be implemented in a simulation-only environment, a HIL implementation would provide performance that is close to a real world scenario.

Also, the need for using HIL test bed is explicitly seen in chapter 4. In a system like GEH, with a high penetration of PVs, the fault current changes over the course of a fault due to the fast exclusion of PVs from the system as per regulatory norms [11].This results in a dynamic shift in the fault current as seen by the protective devices. In the HIL test bed, with the availability of powerful multifunction relays these transients can be efficiently captured and the relay performance under such dynamic conditions can be monitored comprehensively [10]. This justifies the popularity of RTDS as a state of the art simulation test bed for the validation of protection schemes and devices.

REFERENCES

[1] Dr. Hossein Hooshyar, "System Protection for High PV-Penetrated Residential Distribution Systems (Green Hubs)", a dissertation submitted to the North Carolina State University, 2012.

[2] J. Driesen, R. Belmans, "Distributed generation: challenges and possible solutions," proceedings of IEEE 2006 Power Engineering Society General Meeting, 2006.

[3] R.A. Walling, R. Saint, R.C. Dugan, J. Burke, L.A. Kojovic, "Summary of distributed resources impact on power delivery systems", IEEE Transactions on Power Delivery, Volume 23, Issue 3, July 2008, Pages: 1636 – 1644.

[4] A. Girgis, S. Brahma, "Effect of Distributed Generation on Protective Device Coordination in Distribution System", Power Engineering, LESCOPE'01. 2001, Conference on Large Engineering Systems, pp. 115-1 19, 2001.

[5] H. Cheung, A. Hamlyn, L. Wang, C. Yang, and R. Cheung, "Investigations of impacts of distributed generation on feeder protection," in roc. IEEE Power Energy Soc. Gen. Meet., 2009, pp. 1–7.

[6] L.K. Kumpulainen, K.T. Kauhaniemi, "Analysis of the impact of distributed generation on automatic reclosing", proceedings of Power Systems Conference and Exposition. New York: IEEE PES, 2004: 603-608.

[7] M. Baran and I. El-Markabi, "Adaptive over current protection for distribution feeders with distributed generators," in Proc. Conf. Power System and Exposition, 2004, vol. 2, pp. 715–719.

[8] J.A. Silva, H.B. Funmilayo, and K.L. Butler-Purry, "Impact of Distributed Generation on the IEEE Node Radial Test Feeder with Overcurrent Protection". Proceedings of 3911. North American Power Symposium. pp. 49-57, 2007.

[9] David Charles and Ryan McDaniel, “Protection, control And Automation Systems for a multi station looped distribution system”, a manual by SEL.

[10] Seung Tae Cha,Stergaard.J, Qiuwei Wu, Mara.F, ”A real-time simulation platform for power system operation”, IPEC,27-29 Oct.,2010,pp 909-914.

[11] IEEE Std 929-2000, “IEEE Recommended Practice for Utility Interface of Photovoltaic (PV) Systems”.

[12] Relay COMTRADE files location in FREEDM Z drive: Z:\centers\freedm\groups\EPS\Archive-EPS\Bharadwaj\COMTRADE.

[13] RSCAD Simulation files lication in FREEDM Z drive: Z:\centers\freedm\groups\EPS\Archive-EPS\Bharadwaj\RSCAD.

[14] Relay SCD file location in FREEDM Z drive: Z:\centers\freedm\groups\EPS\Archive-EPS\Bharadwaj\Relay.

[15] Nicholas Brooks Parks, “Black Start Control of a Solid State Transformer for Emergency Distribution Power Restoration”, a dissertation submitted to the North Carolina State University, 2012.

APPENDIX

APPENDIX 1: NCSU Notional FREEDM System implementation in Real Time Digital Simulator

The Notional FREEDM system built in PSCAD was based on an actual distribution circuit. This report gives details about the migration of this system to RSCAD. The summary of the PSCAD version can be found in appendix [A] NCSU Notional FREEDM System Report.

System Details:

The Notional System had two feeders operated at 12.47kV. One of those called the Ray Road Feeder has been taken and implemented in the RSCAD. The One Line of the system is attached in the appendix [B]. As per FREEDM lexicon, this is the Green Energy Hub (GEH) -1 system with one of the feeder removed.

System Components:

1. **Substation Transformer:**

The substation transformer details are given below:

Rating: 30MVA, 60Hz, 3ph, DYn1
Voltage: 230/12kV
Leakage inductance: 0.1966pu

The transformer is fed by a source whose details are given below:

230kV, 60Hz, 3ph
X1=0.4126+j5.602 ohms
X0=5.632 at an angle of 85.79885 deg.
Line Sections:

All the Line sections are modeled as PI section models with the line impedances exactly matching the PSCAD versions.

2. Single Phase Subdivision Transformer:

Due to the physical processor availability constraint, The GEH-1 model had one 3ph Transformer serving the distribution loads at each tap. The same has been implemented in the RSCAD. 3 no. of 1ph PVs have been connected to the three legs of the 0.4157kV side of the transformer. All these transformers have the following common configuration:

Rating: 3ph, 60Hz, YnYn
Voltage Rating: 12/0.4157kV

Node	RSCAD Name	3ph MVA
G1	TRF2	0.5
G2	TRF3	2
G4	TRF5	0.2
G5	TR6	6.6

It can be seen that the transformers have been further aggregated with respect to the PSCAD model. This is primarily due to the processor constraint in RTDS (Real Time Digital Simulator). Because of this constraint the No. of PV's have been reduced to 4. The Transformer at node G3 has been removed and the loads attached to this node are being equally fed from Transformers at node G2 and G4. Same is the case with the lateral G5-G9. The transformers in all of these nodes have been aggregated to one transformer at node G5.

3. PV model:

As mentioned before in the GEH-1 system there are single phase PV's attached to the subdivision transformers. The PV model built for the RTDS version is slightly different from the PSCAD version. The photovoltaic panels have been modeled based on the design proposed by Mr. Nicholas Brooks Park in his thesis "Black Start Control of a Solid State

Transformer for Emergency Distribution Power Restoration", chapter 2.7 [C]. Based on the PV panel ratings, the corresponding curve has been built using the MATLAB code [D]. This curve is then fit using the curve fit application in MATLAB with a polynomial curve equation.

In RSCAD a user defined component has been built to solve this polynomial equation which is basically the MPPT output for PV current and voltage. The results for this model are attached in appendix [E].

PV Parameter Settings:

- No. of Parallel cells: 112
- No. of Series cells: 113
- Cell Short circuit Current: 3.83A
- Reverse Saturation Current: 1.2e-7 A
- No. Series PV modules: 4
- No. of Parallel PV modules: 1

APPENDIX 2: PV Model for RSCAD

MATLAB code to generate the polynomial curve fit equation parameters.

```
%*****************************************************************%
% Code: To Generate the Voptimal Vs Suns Curve %
% Written by: Bharadwaj Vasudevan %
%*****************************************************************%
clc
clear all
close all
Iscr=3.83; %cell short circuit current at reference T and S
Irs=1.2e-7; %reverse saturation current
q=1.602e-19; %unit charge constant
k=1.38e-23; %boltzman constant
A=1.92; %ideality factor
K=0.0017; %temperature coefficient
Tr=300; %Reference Temperature
T=273+25; % cell temperature
ns=113; %number of cells in series {round(Voc/0.61)}
np=112; %number of cells in parallel
S=0:0.01:1; %solar radiation
a=(Iscr+K*(T-Tr))*(S/(100*Irs))+1;
b=q/(k*T*A*ns);
Vopt=(lambertw(a*exp(1))-1)/b;
figure(1)
pt1=plot(S,Vopt);
set(pt1,'LineWidth',2)
xlabel('Solar insulation (S)')
```

```
ylabel('V_{optimal}(V)')
title('Optimal Voltage for MPPT')
S1=[0.1 0.5 1];
Iph=0.01.*(Iscr+K.*(T-Tr)).*S1;
vdc=1:1:100;
ipv1=np.*Iph(1)-np.*Irs.*(exp((q.*vdc)./(k.*T.*A.*ns))-1);
ipv2=np.*Iph(2)-np.*Irs.*(exp((q.*vdc)./(k.*T.*A.*ns))-1);
ipv3=np.*Iph(3)-np.*Irs.*(exp((q.*vdc)./(k.*T.*A.*ns))-1);
figure(2)
pt2=plot(vdc,ipv1,vdc,ipv2,vdc,ipv3);
set(pt2,'LineWidth',2)
axis([0 80 0 5])
legend('S=0.1','S=0.5','S=1')
xlabel('V_{dc}')
ylabel('I_{pv}')
title('PV output current Vs PV Terminal Voltage')
ppv1=np.*Iph(1).*vdc-np.*vdc.*Irs.*(exp((q.*vdc)./(k.*T.*A.*ns))-1);
ppv2=np.*Iph(2).*vdc-np.*vdc.*Irs.*(exp((q.*vdc)./(k.*T.*A.*ns))-1);
ppv3=np.*Iph(3).*vdc-np.*vdc.*Irs.*(exp((q.*vdc)./(k.*T.*A.*ns))-1);
figure(3)
pt3=plot(vdc,ppv1./1000,vdc,ppv2./1000,vdc,ppv3./1000);
set(pt3,'LineWidth',2)
axis([0 100 0 0.3])
legend('S=0.1','S=0.5','S=1')
xlabel('V_{dc}')
ylabel('P_{pv}')
title('PV output power Vs PV Terminal Voltage')
```

The PV characteristic curves are shown below in Figure 48 and Figure 49

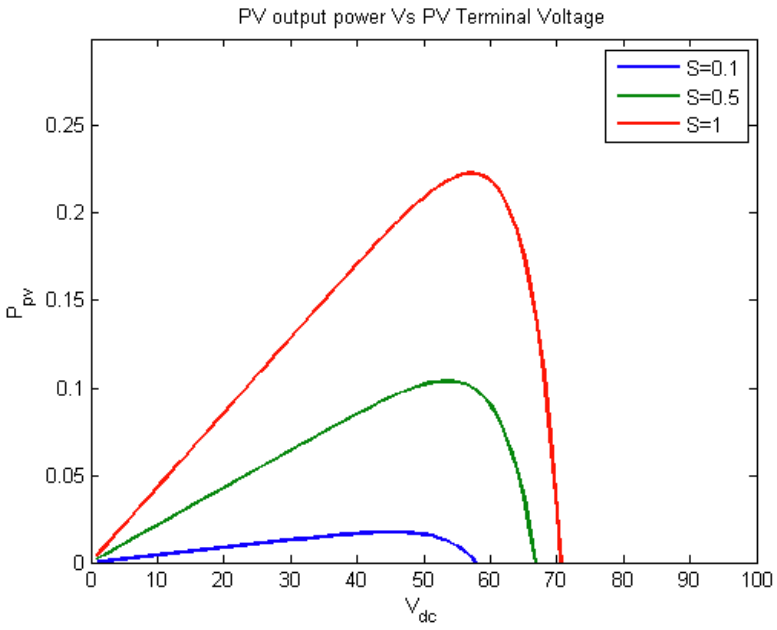

Figure 48 PV Output Power vs. Terminal Voltage

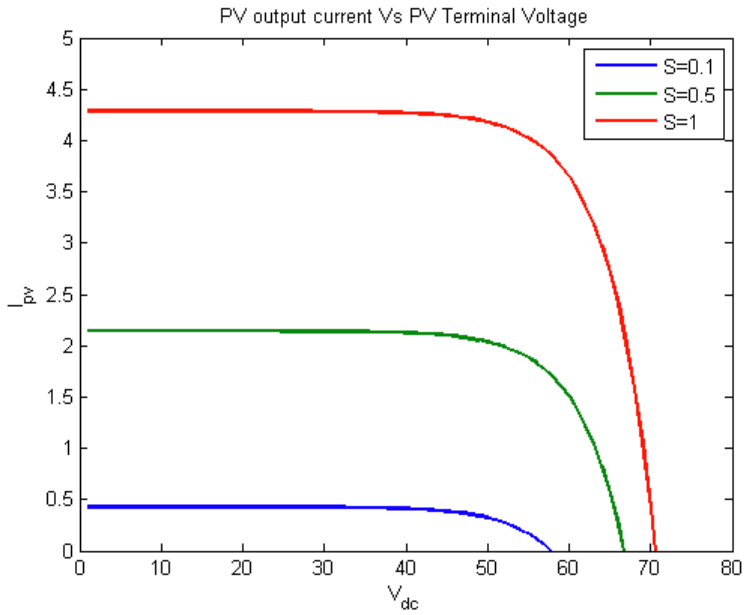

Figure 49: PV V-I Characteristics

APPENDIX 3: C code for the PV Component Model in RSCAD

```
#include "pvcurvefit.h"
STATIC:
/* ---------------------------------------------- */
/* Variables declared here may be used in both the */
/* RAM: and CODE: sections below. */
/* ---------------------------------------------- */
/* double dt; */
double temp,temp1,temp2;
double x;
int l;
double K0,t_tr,Iph;
/* - End of STATIC: Section - */

RAM_FUNCTIONS:
/* ---------------------------------------------- */
/* This section should contain any 'c' functions */
/* to be called from the RAM section (either */
/* RAM_PASS1 or RAM_PASS2). Example: */
/* */
/* static double myFunction(double v1, double v2) */
/* { */
/* return(v1*v2); */
/* } */
/* ---------------------------------------------- */

RAM:
/* ---------------------------------------------- */
```

```
/* Place C code here which computes constants */
/* required for the CODE: section below. The C */
/* code here is executed once, prior to the start */
/* of the simulation case. */
/* ---------------------------------------------- */
/* dt= getTimeStep(); */
K0=0.0017;
t_tr=-2;
/* ---- End of RAM: Section ---- */
CODE_FUNCTIONS:
CODE:
/* ---------------------------------------------- */
/* Place C code here which runs on the RTDS. The */
/* code below is entered once each simulation */
/* step. */
/* ---------------------------------------------- */
//temp1=p1*pow(suns,10)+p2*pow(suns,9)+p3*pow(suns,8)+p4*pow(suns,7)+p5*pow(suns
,6)+p6*pow(suns,5
);
//temp2=p7*pow(suns,4)+p8*pow(suns,3)+p9*pow(suns,2)+p10*suns+p11;
if(polyfit==0)
temp=p1*pow(suns,4)+p2*pow(suns,3)+p3*pow(suns,2)+p4*suns+p5;
if(polyfit==1)
temp=p1*pow(suns,5)+p2*pow(suns,4)+p3*pow(suns,3)+p4*pow(suns,2)+p5*suns+p6;
if(polyfit==2)
temp=p1*pow(suns,6)+p2*pow(suns,5)+p3*pow(suns,4)+p4*pow(suns,3)+p5*pow(suns,2)
+p6*suns+p7;
if(polyfit==3)
```

```
temp=p1*pow(suns,7)+p2*pow(suns,6)+p3*pow(suns,5)+p4*pow(suns,4)+p5*pow(suns,3)
+p6*pow(suns,2)+
p7*suns+p8;
if(polyfit==4)
temp=p1*pow(suns,8)+p2*pow(suns,7)+p3*pow(suns,6)+p4*pow(suns,5)+p5*pow(suns,4)
+p6*pow(suns,3)+
p7*pow(suns,2)+p8*suns+p9;
Vref=nser*temp;
Iph=0.01*(Isc+K0*t_tr)*suns;
Ipv=nsh*np*Iph-nsh*np*Irs*(exp(20.2892*(temp/ns))-1);
//Ipv=40.133*suns-6e-5*(exp(0.079566*(temp))-1);
/* ---- End of CODE: Section --- */
```

APPENDIX 4: ABB Relay Parameter Settings

Settings

Group / Parameter Name	IED Value	PC Value	Unit	Min	Max
ResidualOverCurr4Step(PTOC,51N_67N)					
EF4PTOC: 1					
General					
Setting Group1					
Operation		Enabled			
IBase		650	A	1	99999
VBase		12.00	kV	0.05	2000.00
AngleRCA		65	Deg	-180	180
polMethod		Current			
VPolMin		100	%VB	1	100
IPolMin		100	%IB	2	100
RNPol		5.00	ohm	0.50	1000.00
XNPol		40.00	ohm	0.50	3000.00
INDirPU		100	%IB	1	100
2ndHarmStab		20	%	5	100
BlkParTransf		Disabled			
Use_PUValue		ST4			
SOTF		Disabled			
SOTFSel		Open			
StepForSOTF		Step 2			
EnHarmRestSOTF		Disabled			
tSOTF		0.200	s	0.000	60.000
t4U		1.000	s	0.000	60.000
ActUndrTimeSel		CB position			
tUnderTime		0.300	s	0.000	60.000
Step 1					
Setting Group1					
DirModeSel1		Non-directional			
Characterist1		ANSI Norm. inv.			
Pickup1		73	%IB	1	2500
t1		0.000	s	0.000	60.000
TD1		0.82		0.05	999.00
IMin1		70.00	%IB	1.00	10000.00
t1Min		0.001	s	0.000	60.000
MultPU1		1.0		1.0	10.0
ResetTypeCrv1		ANSI reset			
tReset1		60.000	s	0.000	60.000
HarmRestrain1		Disabled			
tPCrv1		1.000		0.005	3.000
tACrv1		13.500		0.005	200.000
tBCrv1		0.00		0.00	20.00
tCCrv1		1.0		0.1	10.0
tPRCrv1		0.500		0.005	3.000
tTRCrv1		13.500		0.005	100.000
tCRCrv1		1.0		0.1	10.0
Step 2					
Setting Group1					
DirModeSel2		Non-directional			

					Project	Responsible department	Technical ref...	Document kind	Doc. designation
					FREEDM_RTDS(2)	ABB Ltd.			AA1J1Q01A1
				Repla...	FREEDM_RTDS(2).GEH.12kV.Bay1	ABB	Created by	Title REC670	Document id.
Re	Modification	Rel. d...	Creat...	Base...			Approved by		Rev. 0 / Rel. date 4/4/2013 / Lan en / 1 / 3

Group / Parameter Name	IED Value	PC Value	Unit	Min	Max
Characterist2		ANSI Def. Time			
Pickup2		150	%IB	1	2500
t2		0.400	s	0.000	60.000
TD2		0.05		0.05	999.00
IMin2		50.00	%IB	1.00	10000.00
t2Min		0.000	s	0.000	60.000
MultPU2		2.0		1.0	10.0
ResetTypeCrv2		Instantaneous			
tReset2		0.020	s	0.000	60.000
HarmRestrain2		Enabled			
tPCrv2		1.000		0.005	3.000
tACrv2		13.500		0.005	200.000
tBCrv2		0.00		0.00	20.00
tCCrv2		1.0		0.1	10.0
tPRCrv2		0.500		0.005	3.000
tTRCrv2		13.500		0.005	100.000
tCRCrv2		1.0		0.1	10.0
Step 3					
Setting Group1					
DirModeSel3		Non-directional			
Characterist3		ANSI Def. Time			
Pickup3		200	%IB	1	2500
t3		0.800	s	0.000	60.000
TD3		0.05		0.05	999.00
IMin3		33.00	%IB	1.00	10000.00
t3Min		0.000	s	0.000	60.000
MultPU3		2.0		1.0	10.0
ResetTypeCrv3		Instantaneous			
tReset3		0.020	s	0.000	60.000
HarmRestrain3		Enabled			
tPCrv3		1.000		0.005	3.000
tACrv3		13.500		0.005	200.000
tBCrv3		0.00		0.00	20.00
tCCrv3		1.0		0.1	10.0
tPRCrv3		0.500		0.005	3.000
tTRCrv3		13.500		0.005	100.000
tCRCrv3		1.0		0.1	10.0
Step 4					
Setting Group1					
DirModeSel4		Non-directional			
Characterist4		ANSI Def. Time			
Pickup4		300	%IB	1	2500
t4		1.200	s	0.000	60.000
TD4		0.05		0.05	999.00
IMin4		17.00	%IB	1.00	10000.00
t4Min		0.000	s	0.000	60.000
MultPU4		2.0		1.0	10.0
ResetTypeCrv4		Instantaneous			
tReset4		0.020	s	0.000	60.000
HarmRestrain4		Enabled			

Group / Parameter Name	IED Value	PC Value	Unit	Min	Max
tPCrv4		1.000		0.005	3.000
tACrv4		13.500		0.005	200.000
tBCrv4		0.00		0.00	20.00
tCCrv4		1.0		0.1	10.0
tPRCrv4		0.500		0.005	3.000
tTRCrv4		13.500		0.005	100.000
tCRCrv4		1.0		0.1	10.0

Settings

Group / Parameter Name	IED Value	PC Value	Unit	Min	Max
PhaseOverCurrent4Step(PTOC,51_67)					
OC4PTOC: 1					
General					
MeasType		DFT			
Setting Group1					
Operation		Enabled			
IBase		1112	A	1	99999
Vbase		12.00	kV	0.05	2000.00
AngleRCA		55	Deg	40	65
AngleROA		80	Deg	40	89
NumPhSel		1 out of 3			
PUMinOpPhSel		100	%IB	1	100
2ndHarmStab		100	%IB	5	100
Step 1					
Setting Group1					
DirModeSel1		Non-directional			
Characterist1		ANSI Norm. inv.			
Pickup1		100	%IB	1	2500
t1		0.000	s	0.000	60.000
TD1		0.50		0.05	999.00
IMin1		100	%IB	1	10000
t1Min		0.001	s	0.000	60.000
MultPU1		1.0		1.0	10.0
ResetTypeCrv1		Instantaneous			
tReset1		0.020	s	0.000	60.000
tPCrv1		1.000		0.005	3.000
tACrv1		13.500		0.005	200.000
tBCrv1		0.00		0.00	20.00
tCCrv1		1.0		0.1	10.0
tPRCrv1		0.500		0.005	3.000
tTRCrv1		13.500		0.005	100.000
tCRCrv1		1.0		0.1	10.0
HarmRestrain1		Disabled			
Step 2					
Setting Group1					
DirModeSel2		Non-directional			
Characterist2		ANSI Def. Time			
Pickup2		500	%IB	1	2500
t2		0.400	s	0.000	60.000
TD2		0.05		0.05	999.00
IMin2		50	%IB	1	10000
t2Min		0.000	s	0.000	60.000
MultPU2		2.0		1.0	10.0
ResetTypeCrv2		Instantaneous			
tReset2		0.020	s	0.000	60.000
tPCrv2		1.000		0.005	3.000
tACrv2		13.500		0.005	200.000
tBCrv2		0.00		0.00	20.00

Group / Parameter Name	IED Value	PC Value	Unit	Min	Max
tCCrv2		1.0		0.1	10.0
tPRCrv2		0.500		0.005	3.000
tTRCrv2		13.500		0.005	100.000
tCRCrv2		1.0		0.1	10.0
HarmRestrain2		Disabled			
Step 3					
Setting Group1					
DirModeSel3		Non-directional			
Characterist3		ANSI Def. Time			
Pickup3		500	%IB	1	2500
t3		0.800	s	0.000	60.000
TD3		0.05		0.05	999.00
IMin3		33	%IB	1	10000
t3Min		0.000	s	0.000	60.000
MultPU3		2.0		1.0	10.0
ResetTypeCrv3		Instantaneous			
tReset3		0.020	s	0.000	60.000
tPCrv3		1.000		0.005	3.000
tACrv3		13.500		0.005	200.000
tBCrv3		0.00		0.00	20.00
tCCrv3		1.0		0.1	10.0
tPRCrv3		0.500		0.005	3.000
tTRCrv3		13.500		0.005	100.000
tCRCrv3		1.0		0.1	10.0
HarmRestrain3		Disabled			
Step 4					
Setting Group1					
DirModeSel4		Non-directional			
Characterist4		ANSI Def. Time			
Pickup4		500	%IB	1	2500
t4		2.000	s	0.000	60.000
TD4		0.05		0.05	999.00
IMin4		17	%IB	1	10000
t4Min		0.000	s	0.000	60.000
MultPU4		2.0		1.0	10.0
ResetTypeCrv4		Instantaneous			
tReset4		0.020	s	0.000	60.000
tPCrv4		1.000		0.005	3.000
tACrv4		13.500		0.005	200.000
tBCrv4		0.00		0.00	20.00
tCCrv4		1.0		0.1	10.0
tPRCrv4		0.500		0.005	3.000
tTRCrv4		13.500		0.005	100.000
tCRCrv4		1.0		0.1	10.0
HarmRestrain4		Disabled			

					Project	Responsible department	Technical ref...	Document kind	Doc. designation
					FREEDM_RTDS(2)	ABB Ltd.			AA1J1Q01A1
				Repla...	FREEDM_RTDS(2).GEH.12kV.Bay1	ABB	Created by	Title REC670	Document Id.
Re	Modification	Rel. d...	Creat...	Base...			Approved by		Rev. 0 / Rel. date 4/4/2013 / Lan en / 2 / 2